UNIVERSITY POLITEHNICA DIN BUCUREŞTI

FACULTY ŞTIINŢA ŞI INGINERIA MATERIALELOR

PhD THESIS

SUMMARY

INFLUENTA CALITATII OTELURILOR INOXIDABILE CLASA MARTENSITICA ASUPRA DURABILITATII TURBINELOR HIDRAULICE

INFLUENCE OF MARTENSITIC STAINLESS STEEL QUALITY ON HYDRAULIC TURBINES LIFETIME

PhD Advisor:

Prof. Dr. Ing. Cristian PREDESCU

Author:

Ing. George COMAN

CONTENTS

Chapter 1 Current state of knowledge in the field internationally, referring to the most recent references in the specialized literature 4
1.1 Objectives of the research theme 4
1.2 Motivation of the research topic 4
Chapter 2 Study on the corrosion process of steels 5
2.1 Intergranular corrosion (intercrystalline) 5
2.2 Cavitation Corrosion 5
2.3 Corrosion in piting 6
Chapter 3 Research Methodology and Analysis Techniques Used to Achieve Objectives 6
3.1 Purpose and objectives of research 6
3.2 Research Methodology 6
3.3 Experimental Research 7
3.4 Materials used in reasearch 8
Chapter 4 Experimental Investigations on the Time Conduct of Hydroelectric Turbines on the Lower Olt River 10
4.1 Research on the state of the turbine rotor blades at CHE Izbiceni after 16 years of operation .. 10
4.2 Researches regarding the quality of the paddle material of the HA1 Frunzaru director's apparatus, in order to determine the causes that led to the appearance of their prematurely corroded corrosion 12
Chapter 5 Experimental research on improving the quality of steels used in the construction of hydroelectric turbines 18
5.1 Elaboration of steels 18
5.2 Determining the hardness of the prepared steels 20
5.3 Structural investigations by optical microscopy of elaborated steels 20
5.4 Structural and Composite Investigations by Electronic Balloon Microscopy5.4 Structural and Composite Investigations by Scanning Electron Microscopy (SEM) associated with Energy Dispersion Spectroscopy (EDS) 23
Chapter 6 Experimental researches on cavitational erosion resistance and corrosion of elaborated steels 27
6.1 Apparatus used 27
6.2 Corrosion behavior of steels experimented in aqueous environments 29
Chapter 7 Final Conclusions and Original Contributions. New directions of research 32
7.1 Conclusions regarding the structure of the turbine blades from Izbiceni Hydro Power Plant (T8NCuMC130 CS L03.009.0 CCSIT Resita) and from Frunzaru (G-X4CrNi13-4) 32
7.2 Conclusions on the determination of the chemical composition and the elaboration technique for the experimental steels 33
7.3 Conclusions regarding the establishment of thermal treatment parameters 33
7.4 Conclusions on the results of investigations by optical microscopy and electron microscopy... 34
7.5 Conclusions on the results obtained in cavitation erosion testing 34
7.6 Conclusions on the results of the electrochemical corrosion test 34
7.7 New research directions 34
Bibliography 35

Keywords: stainless steel, turbine, martensitic, cavitation, corrosion

Introduction

The main renewable energy source currently used worldwide is that produced by hydropower plants. Although they involve high investment costs, they have the advantage of using water, the virtually inexhaustible resource. The current technology has made it possible to optimize the turbines with high mechanical performance and performance, with the main problems left to be solved by their maintenance.

In a hydroelectric plant, turbine components have the greatest exposure to damage, and the factors that lead to this result are related to water trail and water quality, turbine kinematics and dynamics, and operating regime.

The main causes contributing to increased service periods for repairs are the occurrence of cracks and erosion at the rotor and blades. These are generated by defects in material or manufacturing, fatigue or overload. Erosion is caused by the sand trained in the turbine together with water as well as by the phenomenon of hydrodynamic cavitation (cavitation erosion). Cavitational erosion craters often have depths of the order of millimeters. Thus, it is sometimes possible to perforate the affected areas in the case of hydraulic turbine blades, which are the most affected by cavitation erosion.

The paper contains 7 chapters, contains 155 pages, original conclusions and contributions as well as the bibliography.

Chapter 1 presents the objectives and motivation of the research theme, the theoretical study of the erosion - corrosion mechanism of the rotors of the hydropower turbines, a classification of the used materials and the technologies for their realization.

In Chapter 2 are presented the contributions to the study of the corrosion process of the steels, intergranular corrosion (intercrystalline), cavitation corrosion and corrosion in pitting.

The research methodology and analysis techniques used to achieve the objectives are presented in Chapter 3.

Chapter 4 presents the experimental research carried out comparatively on samples taken from the turbine blades from the Frunzaru Hydroelectric Power Plant, which were prematurely depreciated after two years of operation (upgraded) and Izbiceni Hydro Power Plant after more than 25 years of operation.

Chapter 5 presents experimental research on improving the quality of steels used in the construction of hydroelectric turbines. Three martensitic stainless steels were developed in vacuum and controlled atmosphere. The three elaborated steels were subjected to thermal treatments, after which they were structurally characterized and tested for resistance to corrosion and cavitation.

Chapter 6 Analysis of the cavitation and corrosion behavior of the elaborated steels.

Chapter 7 presents the final conclusions, the original contributions and the new research directions.

Chapter 1 Current state of knowledge in the field internationally, referring to the most recent references in the specialized literature

1.1 Objectives of the research theme

The research topic proposed in this paper aims at:

• Contributions to the mechanism of the cavitation and pitting corrosion process in hydropower turbines;

• Establishing the causes that led to the premature degradation of the turbine blades from the Olt river hydropower plants after their upgrade;

• Design, manufacture and characterization of new materials with improved properties for the construction of hydroelectric turbines;

1.2 Motivation of the research theme

Hydropower constructions are considered to be energy aggregates of national, regional and even global interest, given the economic role of electricity supplier in national or regional systems, the role of potential energy reservoir, the ecological role of pluvio-fluvial regulator, and the role of actor in the process of sustainable development of the society as a supplier of renewable, low-polluting energy.

Chapter 2 Study on the corrosion process of steels

In the case of stainless steels, the literature shows three types of corrosion: intercrystalline, cavitational and pitting.

Frankel et al. [72] have provided as critical factors the effect of alloy composition, the potential value and the temperature at which corrosion occurs. Possible factors involved in corrosion are shown in Figure 2.1. These factors are: (1) physical factors (2) chemical factors (3), biological factors and (4) metallurgical factors. The factors that can affect the corrosion in the points in Figure 2.1 are composed of all types of exposure areas. Influence factors are not limited only to stainless steels, light and low alloy steels being also taken into account, the literature showing similar corrosion behavior [73]; [74]; [75].

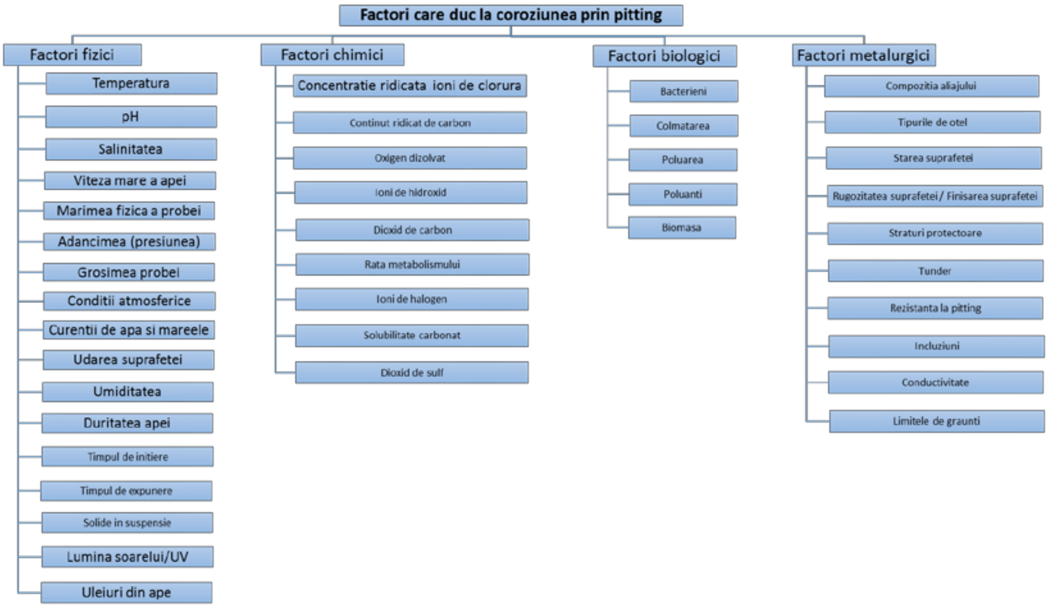

Fig. 2.1. Factors that can affect point corrosion

2.1. Intergranular corrosion (intercrystalline)

Intercrystalline corrosion is the type of preferential corrosion of the grain boundaries of metallic materials. This phenomenon occurs in the absence of mechanical stresses. In the case of intergranular corrosion, the mass loss of the material is not significant, but the change in the mechanical characteristics. In some cases, the intensity of the corrosive attack is so great that the material breaks into separate granules, losing its total mechanical strength.

The corrosion phenomenon involves two stages: one initiation stage and one propagation stage. The determinants of the two stages are often quite different. For localized corrosion reactions, the initiation step is strongly influenced by the structure of the material [76].

The preferential destruction of the grain boundaries is due either to their more active character due to their associated energy, or to the separation of some phases, usually intermetallic complexes with electrode potential different from that of the matrix in the case of pure metal or a homogeneous solution, without precipitation, the intergranular corrosion phenomenon is harder to observe. Its occurrence in this case may be due to the grain boundary structure.

2.2 Cavitational corrosion

Cavitation corrosion is a particular form of erosion caused by the implosion of gas bubbles on a metallic surface. Corrosion erosion and cavitation corrosion, including erosion corrosion, are processes that combine mechanical wear with the effect of severely destroying equipment subject to these demands. The combination of mechanical erosion and the presence of a corrosive environment can have a significant effect on the life of a piece. In corrosion erosion and cavitation corrosion, erosion and wear increase the corrosion rate of a piece by destroying the protective film or the cover from its surface.

2.3 Pitting corrosion

Pitting corrosion is described as a localized corrosion of the metal surface limited to a reduced area or a point that takes the form of a cavity [106]. The major consequences of pitting are mainly related to the destruction of passivation because it appears on the surface of films who are exposed to aggressive environment, when discrete areas of the material are quickly attacked, while neighboring surfaces remain unattacked [107]. The attack leads to characteristic shapes of the cavity, such as pits or crevices in the surface of the material [108].

Corrosion in pitting is of particular importance where steel structures involve high pressure operation, boilers, turbine blades, metallic containers for toxic materials.

Corrosion in pitting can cause holes to exterior "open" (can not close) or can be coated with semi-permeable membranes of corrosion products. The holes can be either hemispherical or cup-shaped. In some cases, they are flat, flat walls, indicating the crystal structure of the metal, but may also have an irregular shape.

Chapter 3 Research methodology and analysis techniques used to achieve the objectives

3.1. Purpose and objectives of the research

The purpose and objectives of the research are:

- Evaluation of existing data in the literature on the steels used in the construction of hydroelectric turbines;
- Establishing the causes that led to the premature degradation of turbine blades from the Olt river hydropower plants after their upgrade;
- elaboration of three types of martensitic and austenitic-martensitic stainless steels, to be used in the production of hydroelectric turbines;
- physico-mechanical characterization of the three steels;
- Determination of cavitation erosion behavior;
- Determination of corrosion resistance;
- Dissemination of research results so as to ensure the practical exploitation of steels designed;

3.2. Methodology of research

The research carried out in this paper has been developed using as a working tool a complex of principles, processes and techniques with the role of expanding the scientific knowledge and efficiently solving the practical problems related to the efficient use of hydropower turbines.

The research methodology has as its starting point the current state of research in the field, as it is found in the literature. Thus, the influence of cavitational corrosion on the lifetime of energy equipment is not yet fully scientifically substantiated. The necessity to become a research subject is already underlined by the cases observed during the operation of the refurbished turbines on the Olt river. It has been found that these require immediate solutions and interventions regarding the quality of the materials used and the technology for their realization in order to increase the resistance to cavitation corrosion.

On the basis of the above, the research plan was drafted in view of the following aspects:

1) To justify the need to approach such a research topic as a major subject of material science, with emphasis on the behavior of hydroelectric turbine materials at cavitation corrosion;

2) Contributions to the development and improvement of the stainless steel manufacturing technologies used in the construction of hydroelectric turbines.

This objective seeks to scientifically substantiate the possibilities of defining, elaborating and processing of stainless steel alloy materials used in hydroelectric constructions in order to improve their quality. Within this framework, topics such as:

a) The current state of knowledge in the field internationally, referring to the most recent references in the literature

b) Mechanism of the cavitational, intercrystalline and pitting corrosion process

c) Creating new materials with specified composition to optimize the erosion-corrosion behavior;

d) Testing materials simulating the most severe operating conditions for hydroelectric turbine blades;

e) Critical association of research results.

3) Research on the development of technologies and techniques for obtaining corrosion-resistant materials, focusing on the following aspects:

a) Experimental research on the time behavior of hydropower turbines on the river Olt

b) Experimental research on improving the quality of steels used in the construction of hydroelectric turbines

4) Original contributions and research directions.

3.3. Experimental research

The experimental researches are summarized in Figure 3.1 and include the comparative analysis of the turbines from CHE Frunzaru and CHE Izbiceni, after which the causes that contributed to the premature damage of the turbine blades from CHR Frunzaru were determined. Following the conclusions of the metallurgical investigations, two stainless steel batch commonly used in the manufacture of turbine blades and an innovative steel batch with high cavitation and corrosion properties were made.

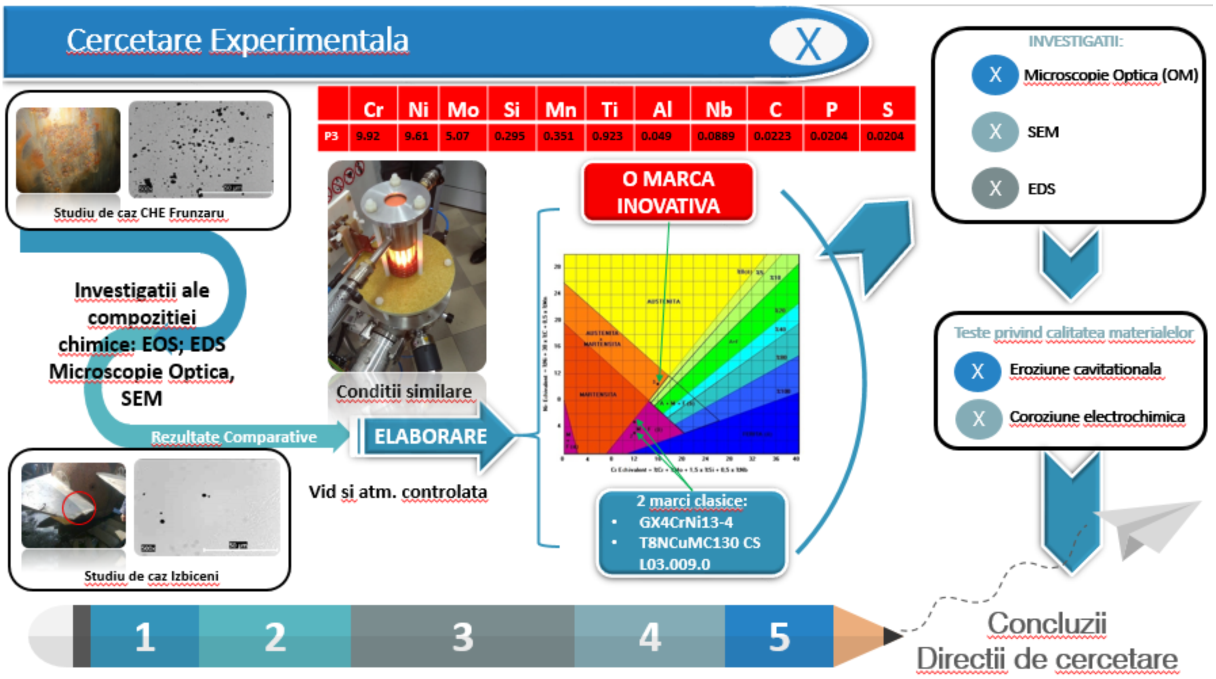

Fig 3.1 The schematic representation of the experimental researches

3.4. Materials used in research

In the research two categories of materials were studied:

- stainless steel from hydroelectric turbines on the Olt River;
- austenitic - martensitic stainless steels and ferrite - martensitic developed in the UPB-ECOMET laboratories in order to obtain materials with improved properties due to the deficiencies observed during the study of materials from hydroelectric turbines.

3.4.1. Sampling of the Izbiceni and Frunzaru hydropower plants

For investigations on the technical state of the turbines on the Olt river, we used samples taken from blades from the Izbiceni and Frunzaru hydropower plants made of martensitic stainless steel. Samples were manually cut by cross-section and longitudinal sectioning. During the sampling, overheating was avoided.

a) b)

Fig. 3.2. Sampling of hydroelectric turbines on the Olt river a) Izbiceni b) Frunzaru

3.4.2. Elaboration of stainless steels for experimental research

The stainless steels used for the experimental research have been developed in a cold-crucible furnace, with vacuum and argon atmosphere, such as the Fives Celes ALU 600.

The steps taken to make stainless steel samples were:

1. Prepare and calculate the furnace load in order to position the three elaborated stainless steel brands in the Schaeffler diagram.

Cr_{ech} and Ni_{ech} have been computed with the relationships:

$$Ni_{ech} = \%Ni + 30x\%C + 0,5x\%Mn; \quad Cr_{ech} = \%Cr + \%Mn + 1,5x\%Si + \%Cb.$$

3 Elaboration and casting of steels in cooled copper ingots.

Fig. 3.3. Cold-crucible furnace, with vacuum and argon atmosphere

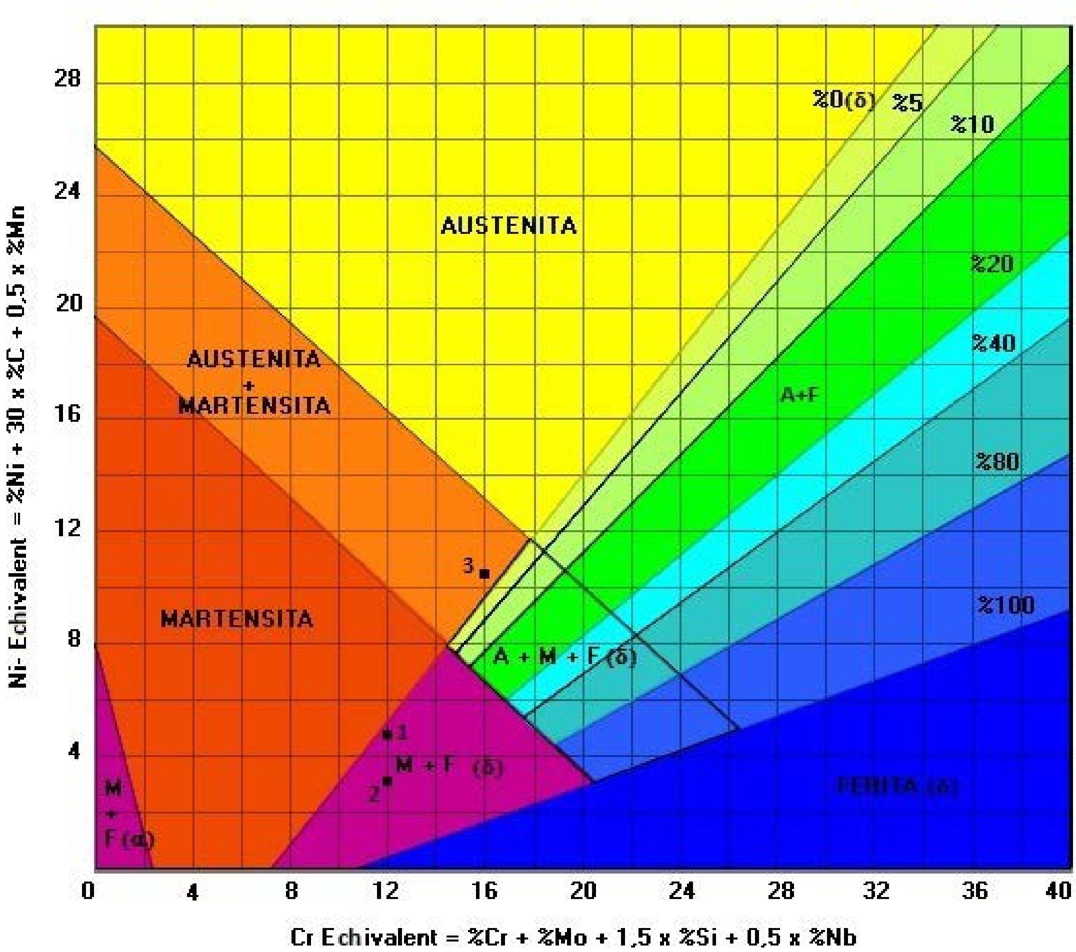

Fig. 3.4. Positioning in Schaeffler diagram of steels developed for experimental research

Chapter 4 Experimental researches on the behavior of hydroelectric turbines on the lower Olt river

Hidroelectrica started the process of modernization of the hydroelectric units on the lower Olt river in 2006, when the maximum power available at the plant level was 37MW due to power constraints caused by technical problems. The most frequent events demonstrating deficiencies in the operation of the energy groups are in particular: gulking of the turbine bearing, excessive heating of the generator winding due to the defective ventilation system, modification of the generator stator shape with disturbance of the gap, gripping of the head at the distribution head, breakage of the turbine shaft, damage to the blade surface due to cavitation corrosion and pitting, breakage of the turbine rotor blades.

Such defects occur even at partial loads. To increase the duration of the groups, between two consecutive incidents, it is common for them to be operated with partial loads and to permanently monitor the evolution of certain status parameters of the groups. Even in this situation, mechanical or electrical deficiencies may occur causing a large number of hours of accidental shutdown of the groups.

Upon re-engineering, the maximum available power increased to 57 MW on CHE (an increase of 14.25 MW / group).

4.1. Research on the state of the turbine rotor blades at CHE Izbiceni after 16 years of operation

In order to analyze the state of the turbine material at Izbiceni, samples were taken from the HA1 palette. The appearance of the HA1 rotor blade is shown in Figure 3.1 a.

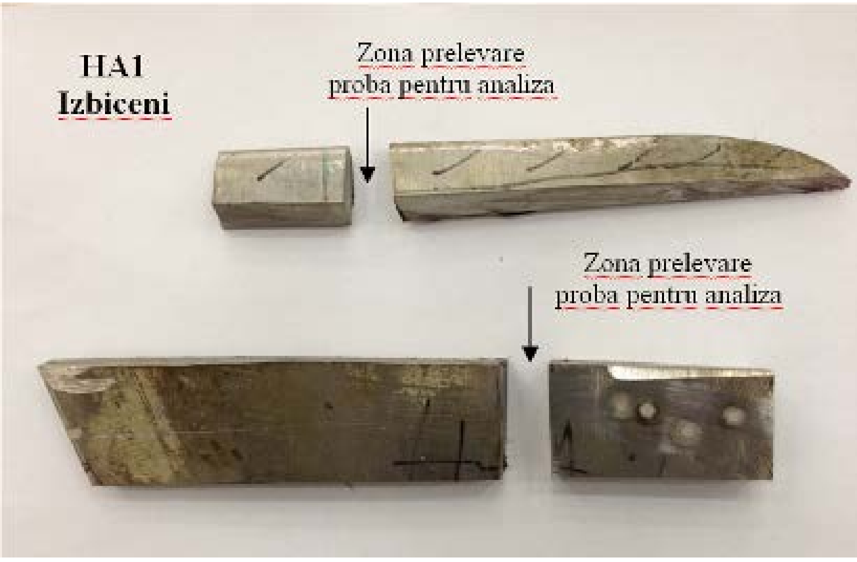

Fig. 4.1. The appearance of the sampling areas analyzed

The investigations carried out on samples taken from the rotor blade from HA1 Izbiceni consisted of:

- Determination of the chemical composition by the optical emission spectrometry method;
- Determining the hardness of the material;
- Metallographic analysis by optical microscopy;
- Microstructural and micro-compositional analysis.

4.1.1. Obtained results

The values obtained from the determination of the chemical composition are presented in Table 4.1:

Table 4.1 Chemical composition of the material

Marca/ Norma	Continutul în %									
	C	Si	Mn	P	S	Cr	Ni	Mo	Cu	V
Paletă rotor vechi HA1 Izbiceni	0,074	0,332	0,595	0,016	0,022	13,453	1,325	0,066	1,295	0,029
T8NCuMC130 CS L03.009.0 CCSIT Reşiţa	max. 0,10	max. 0,4	0,2÷ 0,6	max. 0,025	max. 0,030	12,0 ÷ 13,5	1,0÷ 1,5	-	1,0÷ 1,3	-

The results of the hardness measurement measurements made on the surfaces of samples from the HA1 Izbiceni old rotor blade are shown in Table 2.

Table 4.2. Hardness values HV10

Nr. crt	Denumire probă	Valori măsurate [HV10]	Media
1	Paletă rotor vechi HA1 Izbiceni	250; 235; 241	242

4.1.2. Metallographic analysis by optical microscopy

Samples prepared for examination, unattacked with metallographic reagents, indicate the presence of oxidative and sulphide inclusions in the mass of the material having a circular and / or elliptical shape of randomly distributed micrometric sizes (Figure 4.4). No microvoids, microsprays or pores were found in the base mass of the analyzed samples.

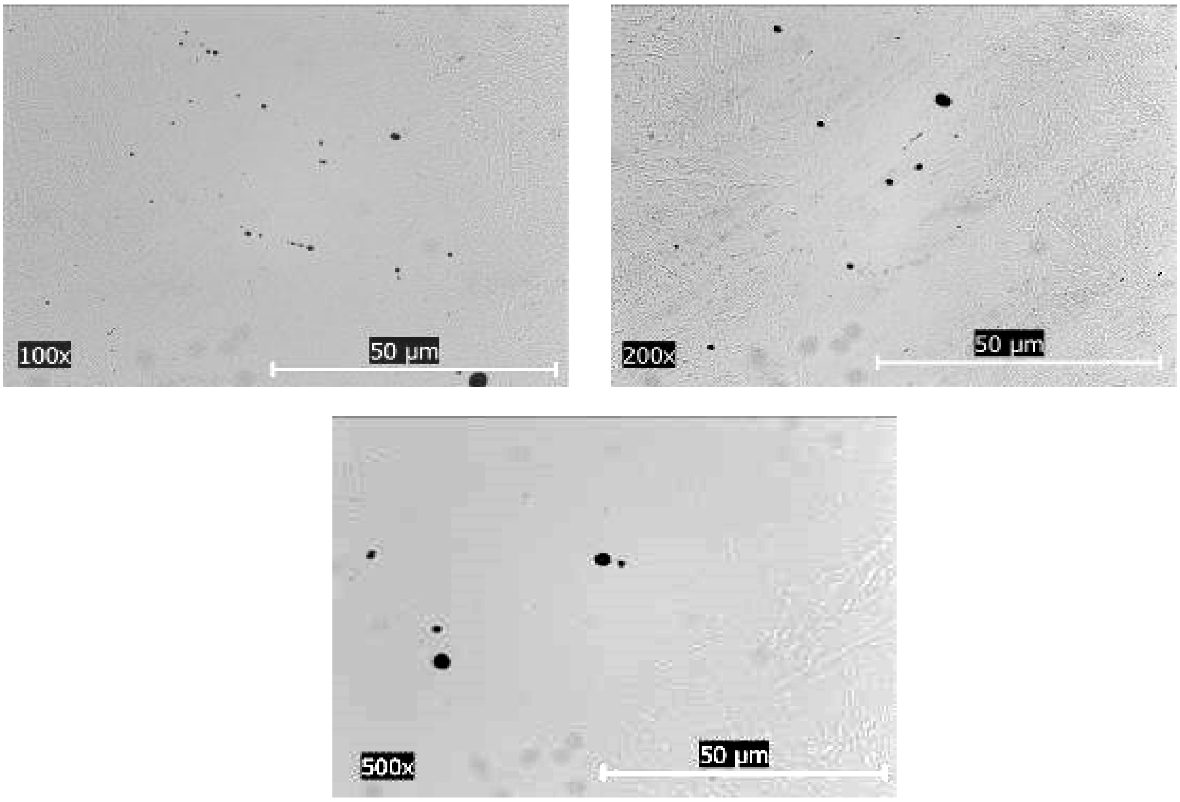

Fig.4.2. The appearance of the metalographic microstructure in the samples from the palette

b) Samples prepared for examination, attacked with metallographic reagents (Marble Reagent), previously analyzed, were examined at a 100X magnification. The metallographic structure is typical for the determined steel brand, its appearance is shown in Figure 4.5.

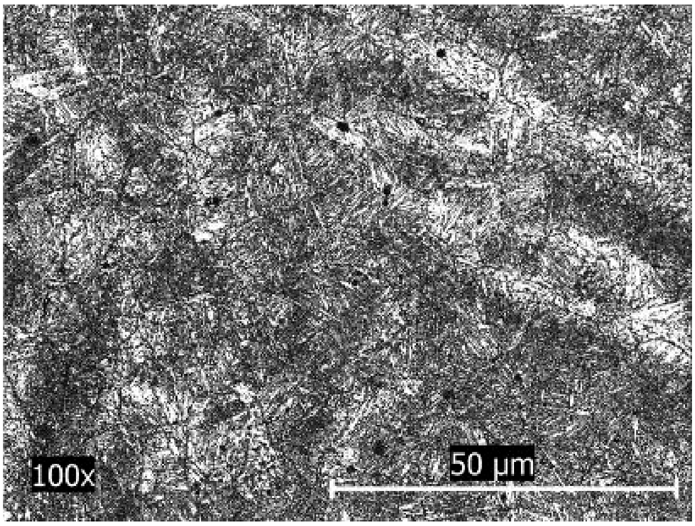

Fig.4.3. The aspect of the metallographic structure corresponding to a treatment quenching and tempered

4.1.3. Microstructural and microcompozitive analysis

The microstructural and micro-compositional investigation of the samples was performed by scanning electron microscopy (SEM) and by energy-dispersive X-ray microanalysis (EDAX) on the Quanta Inspect F scanning microscope.

The microstructural and micro-compositional analysis of the extracted material determined the nature and size of inclusions observed in the optical microscope present in the structure of the material.

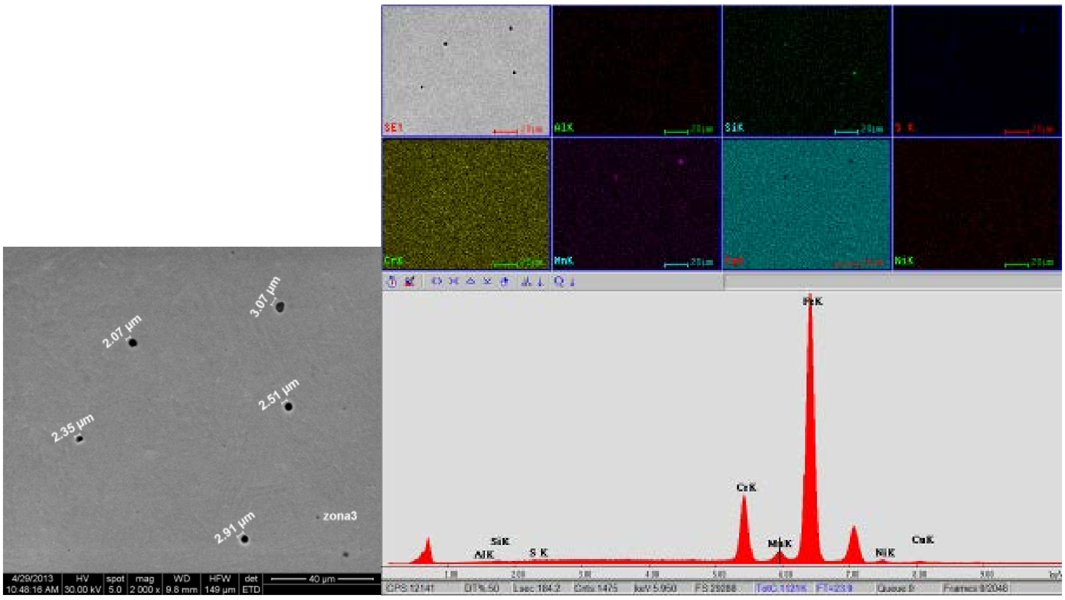

Fig. 4.4. Scanning Electron Microscopy (SEM) image at a 2000x magnification showing the presence of micrometric inclusions of manganese sulfide and the dispersive X-ray spectrum in energy (EDAX) and the distribution of the homogeneity of the elements in the micro area presented

4.2. Research on the quality of the blades material of the HA1 Frunzaru turbine, in order to determine the causes that led to the appearance of a significant premature corrosion

Three years after the refurbishment of CHE Frunzaru, an early corrosion was observed. In this case, the research aimed at assessing the quality of the materials from HA1 Frunzaru in order to determine the causes that led to their degradation. [162]

The activity was also carried out in the laboratories of the Center for Research and Eco-Metallurgical Expertise at POLITEHNICA University in Bucharest (ECOMET).

The appearance of the blade affected by corrosion is shown in Figure 4.8.

Fig. 4.5. Appearance of the corroded surface of the pallet

Samples 1 and 2 were taken from the corrosion-affected area (Figure 4.3) and samples 3 and 4 were taken from the edge of the blade (Figure 4.16).

Fig. 4.6. Samples taken from the turbine rotor blade

4.2.2. Obtained results

The values resulting from the determination of the chemical composition are shown in Table 4.3:

Table 4.3. Chemical composition of the material

Marcaj Probe	**Elemente %**										
	C	**Si**	**Mn**	**P**	**S**	**Cr**	**Mo**	**Ni**	**V**	**Al**	**Cu**
6	**0,030**	**0,39**	**0,70**	**0,030**	**0,001**	**12,47**	**0,43**	**3,80**	**0,03**	**0.014**	**0,20**
G-X4CrNi13-4	**<0,06**	**<1**	**<1**	**<0,035**	**<0,025**	**12-13,5**	**0,4-1**	**3,5-4,5**	**-**	**-**	**-**

Steel is in the G-X4CrNi13-4 class or ASTM A743 / A743M (2003) CA6NM class.

Measurements for determining the hardness were made on the surfaces of sample as well as on the surface studied in the metallographic analysis from the blade body. The results of the measurements are shown in Table 4.4.

Table 4.4. Hardness values HV10

Nr. crt	Denumire probă	Valori măsurate [HV10]	Media
1	Corp probă marcaj 6	285; 281; 324	297

4.2.3. Metallographic analysis by optical microscopy and electron microscopy

a) Samples prepared for examination, unattacked with metallographic reagents, indicate the generalized presence of material discontinuities of randomly distributed circular and / or elliptical shape of the material, representing oxidative and sulphide inclusions associated with coarse microsprays / microporouss (Figure 4.10) .

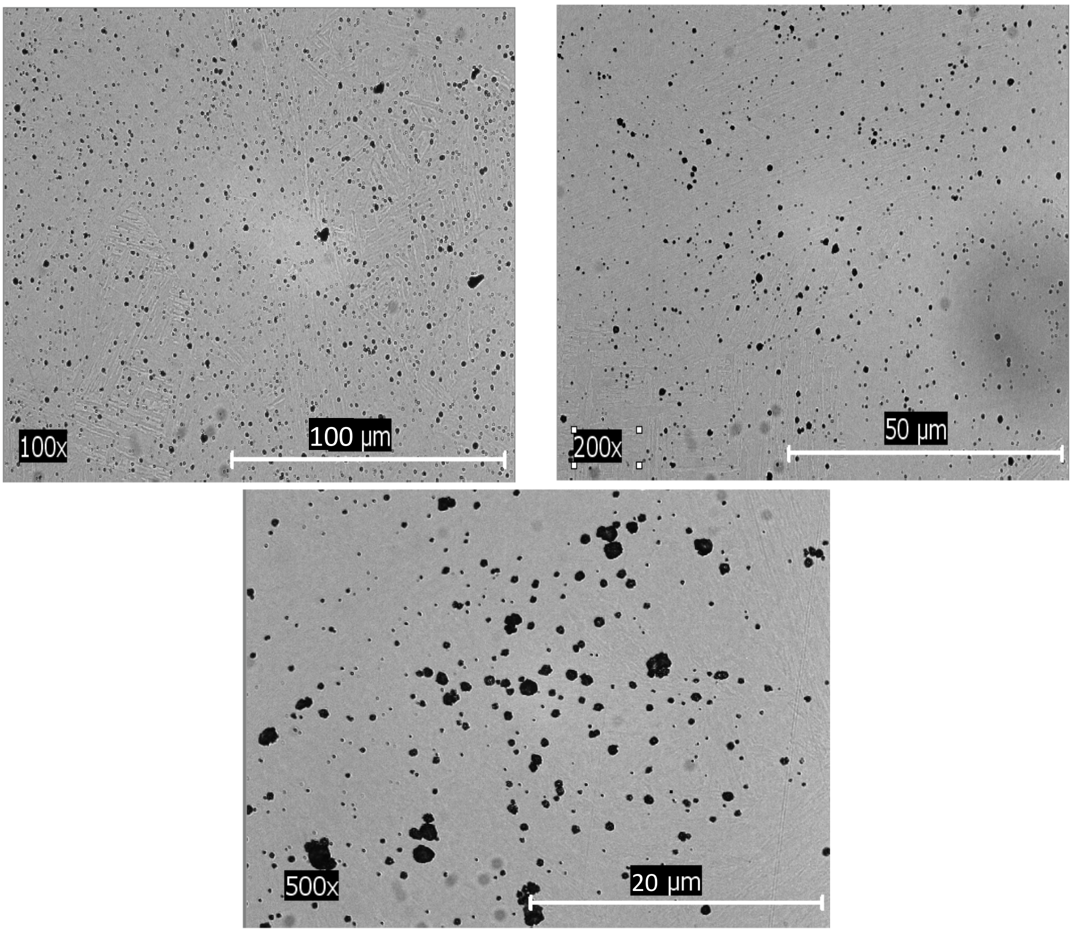

Fig. 4.7. The appearance of the metallographic microstructure in the samples from the blade

b) Samples prepared for examination, attacked with metallographic reagents (Marble Reagent), previously analyzed, were examined at a 100X magnification. The metallographic structure is typical of the determined steel brand, its appearance being shown in Figure 4.11.

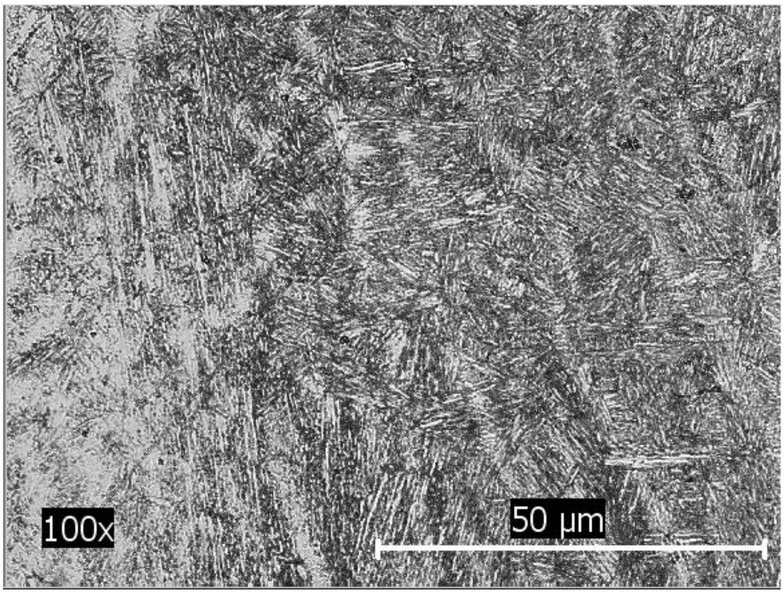

Fig. 4.8. The appearance of the metallographic structure corresponding to a quenching and recovery treatment

The microstructural and micro-compositional investigation of the samples was performed by scanning electron microscopy (SEM) and by energy-dispersive X-ray microanalysis (EDAX) on the Quanta Inspect F scanning microscope.
The microstructural and micro-compositional analysis of the collected material resulted in a series of discontinuities in the structure of the material, which can be grouped as follows: aluminum oxides, manganese sulphides, microspheres and microrecipients.

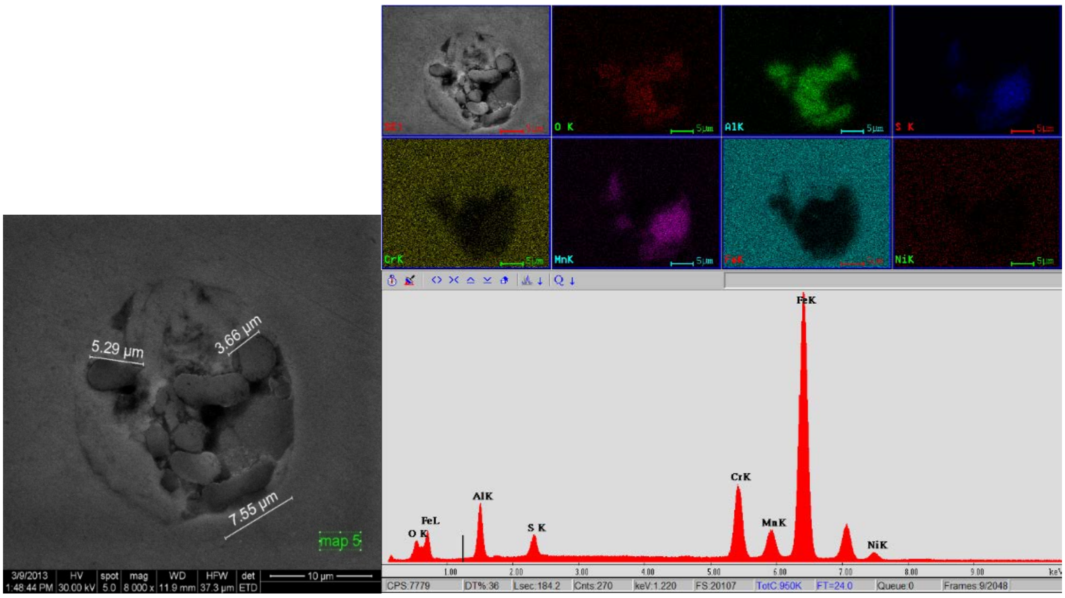

Fig. 4.9. Scanning electron microscopy (SEM) image at an 8000x magnification showing the appearance and presence of manganese sulphides and aluminum oxides and the dispersive X-ray energy spectrum (EDAX) and the distribution of the homogeneity of the elements in the presented microarea

At the bottom of the image is the energy dispersive X-ray spectrum (EDAX) obtained on the microarea in Figure 4.12. We observe the presence of the elements: O, Fe, Al, S, Cr, Mn, Ni; In the upper left corner of the image, the aspect of the analyzed microarea is highlighted; the other frames of the image show the X-ray distribution of the elements present in the analyzed microarea. This highlights the presence of a complex inclusion of manganese sulphides and oxides of aluminum.

4.2.4. Evidence of gas holes and microholes in the analyzed sample

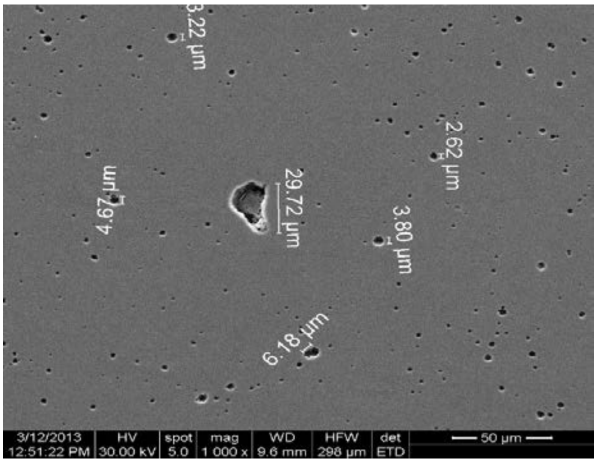

Fig. 4.10. Microholes and gas holes present in the analyzed sample

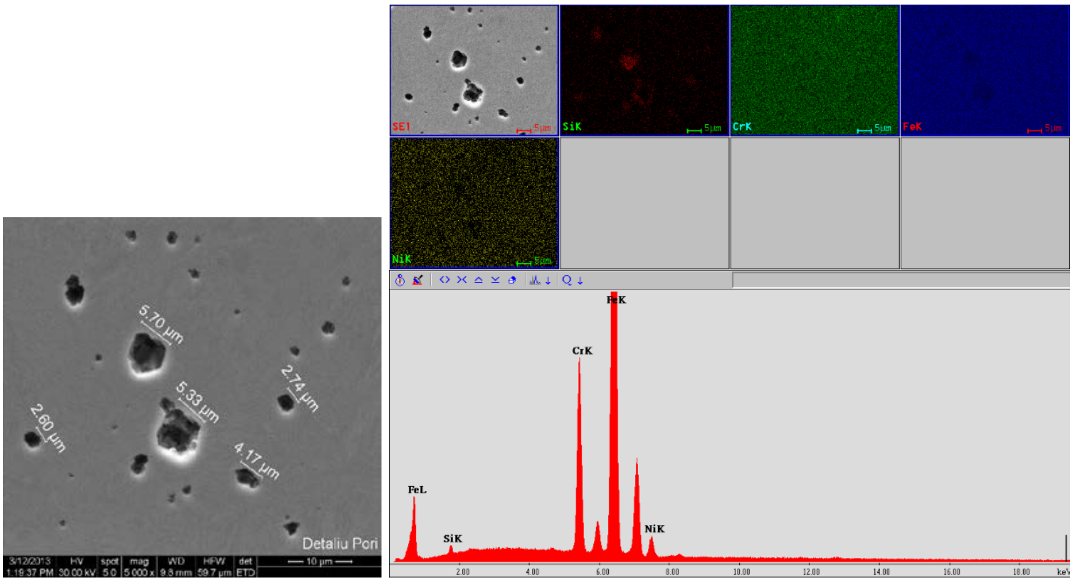

Fig. 4.11. The energy dispersive X-ray spectrum (EDAX) and the homogeneity distribution of the elements in the presented micro area

At the bottom of the image, the energy dispersive X-ray spectrum (EDAX) obtained on the micro area in Figure 4.26 is highlighted. The presence of these elements in the micro are is observed: O, Fe, Si, Cr, Ni; In the upper left corner of the image, the aspect of the analyzed micro area is highlighted; the other frames of the image show the X-ray distribution of the elements present in the analyzed micro area. The homogeneous distribution of the elements demonstrates that the structural defects present in Figure 4.26 are not inclusions but micro gas holes / micropores in the material, identifying traces of Si at the material interface.

4.2.5. Conclusions

1. The chemical composition of steel corresponds to a steel grade GX4CrNi13-4 EN 10283, or ASTM A743 / A743M (2003) CA6NM, martensitic stainless steel, indicated by the literature for the execution of hydraulic turbine rotors;

2. The metallographic structure resulting from the optical microscopy analysis on the Marble Reagent-stained sample is typical of the determined steel mark resulting from thermal quenching and tempering;

3. Electron microscopy analysis reveals the presence of MnS inclusions ranging between 4 and 20 μm, inclusions and networks of aluminum oxides with dimensions between 3 and 90 μm, complex inclusions of manganese sulphides and aluminum oxides with sizes between 10 and 37 μm, as well as multiple micro-closures and micropores with sizes between 2 and 29 μm;

4. The presence of sulphides and oxides inclusions is a potent factor for the initiation of localized pitting or creep corrosion in stainless steels, the surface of which passes through the formation of a protective oxide layer. The passivated area represents the cathodic area, and the inclusions represent the anode area.

Chapter 5 Experimental research on improving the quality of steels used in the construction of hydroelectric turbines

5.1. Steel production

The elaboration of the stainless steels subjected to the research was done in an induction furnace with a cold copper crucible with an inner diameter of at least 35 mm and the capacity of min 8 cm3 and max 15 cm3 equipped with a casting plug, figure 3.2. The operating parameters of the furnace are: nominal power 25 kW, frequency HF 100 - 400 kHz, apparent power 40 kVA, phase current 40 A, power factor 0.92, minimum water flow 12 l / min, maximum inlet pressure: 7,5 bar, water inlet temperature: max. 24 ° C. The maximum working temperature of the oven is 2800 ˚C and the vacuum system contains a primary vacuum pumping station including a pump of at least 1.7 m3 / h with a vacuum limit of 10^{-4} mbar and a vacuum pump pumping station: $1x10^{-8}$ mbar.

Fig. 5.1. Stainless steel ingots made in the induction furnace with a cold crucible

The calculation of the load was made so as to obtain three steel billets, Figure 5.1, with the chemical composition shown in Table 1 and whose positioning in the Schaeffler diagram is shown in Figure 5.2.

In P3 steel, small amounts of Ti (0.92%), [172] were also added. The model was taken from the chemical composition of maraging steels, with which it is related. According to references [163] and [164.] in maraging steels, Ti it is present because it favors precipitation of Ni_3Ti compounds, which together with Ni_3Co compounds, generates the highest hardening effect. The dosage of Ti must be reduced to lower levels because the hardening mechanism involved induces a strong internal stress at the crystalline level which could influence the corrosion resistance imposed on the new steel. Taking into account the data from the literature, the option was directed to a minimum value of ~ 0.9%.

Table 5.1 Three bits, P1, P2, P3, have been developed with the following compositions:

	Cr	**Ni**	**Mo**	**Si**	**Cu**	**Mn**	**Ti**	**Al**	**Nb**	**C**	**V**	**Co**	**P**	**S**	**Fe**
P1	**11.78**	**4.34**	**0.002**	**0.182**	**0.078**	**0.550**	**0.001**	**0.0061**	**0.012**	**0.042**	**0.025**	**0.016**	**0.0079**	**0.0085**	**82.95**
P2	**12.05**	**3.85**	**1.024**	**0.393**	**0.170**	**0.676**	**0**	**0.0282**	**0.0438**	**0.0426**	**0.0081**	**0.0299**	**0.0287**	**0.0114**	**81.64**
P3	**9.92**	**9.61**	**5.07**	**0.295**	**0.147**	**0.351**	**0.923**	**0.049**	**0.0889**	**0.0223**	**0.0022**	**0.0356**	**0.0204**	**0.0204**	**73.8**

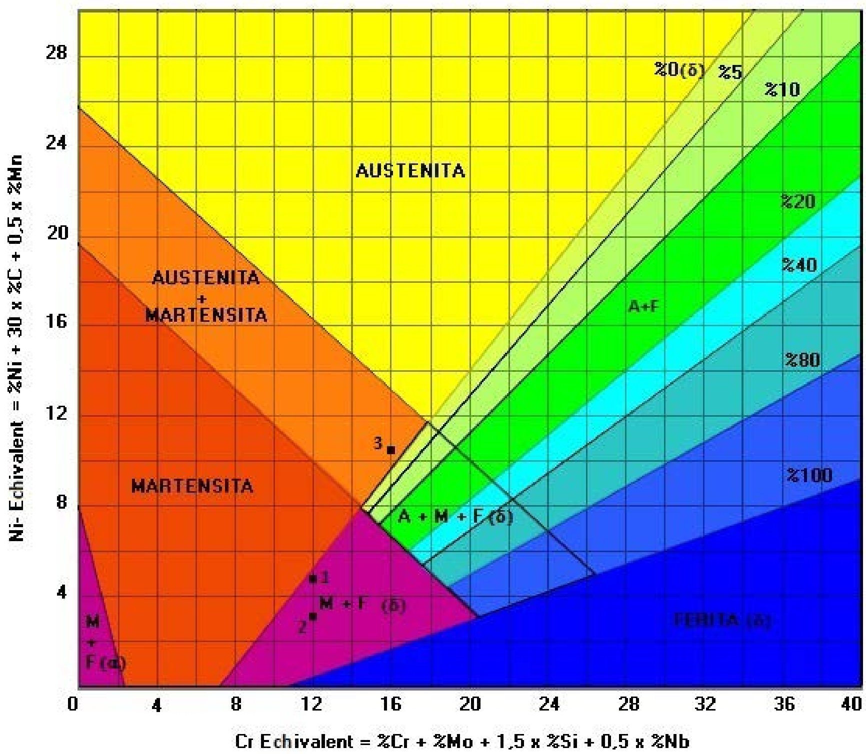

Fig. 5.2. Positioning in the Schaeffler diagram of the three stainless steel brands developed for experimental research

The elaborated steels were characterized in terms of hardness, metallographic structure, corrosion and cavitation resistance.

5.2. Hardness determination of developed steels

Determination of the hardness of the three steels was done with the help of an Innovatest automatic hardness tester, the results of the sample measurements in all phases (cast, quality, return) are presented below:

For example, in table 5.2, the average hardness values obtained after elaboration / casting, quenching, tempering will be synthesized.

Table 5.2 Average hardness values obtained after elaboration / casting, tempering

Proba	HV elaborat/turnat	HV calit	HV revenit
1	382	349	279
2	355	343	318
3	308	315	486

For samples 1 and 2, the hardness after tempering returns lower values than after quenching. The decomposition of martensite in heating, with the elimination of internal tensions, contributes to this phenomenon, evoking a sequence of transformations similar to those that appear in the classic mode of return.

In case of sample 3, we see an increase in hardness from 315 HV to 486 HV, in a multiplication of almost 1.6 times. We place these results on the occurrence of precipitates that occur and which increase hardness on the basis of the "hardening by precipitation" mechanism, a particular case of "dispersing hardening". This is the fundamental phenomenon of the decomposition of supersaturated solid solutions, the basis of the thermal treatment of aging. [172]

5.3. Structural investigations by optical microscopy of elaborated steels

The first step in the structural investigation of the studied steels included optical microscopy. The analysis method requires two preliminary operations, followed by the microscopic analysis itself. This was done:

5.3.1. Structural investigations of samples obtained after elaboration and casting

In the series of micrographs in Figures 5.3, 5.4 and 5.5 are presented the structures of the three steels after casting

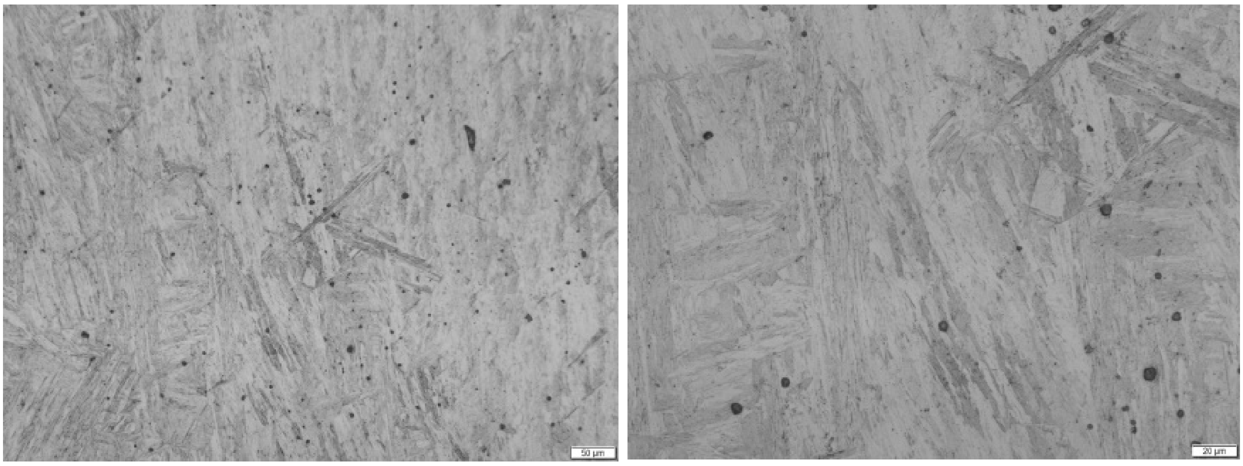

a b

Fig. 5.3 Optical microscopy images for sample 1 results after casting 200x (a) 500x (b); Marble attack reagent

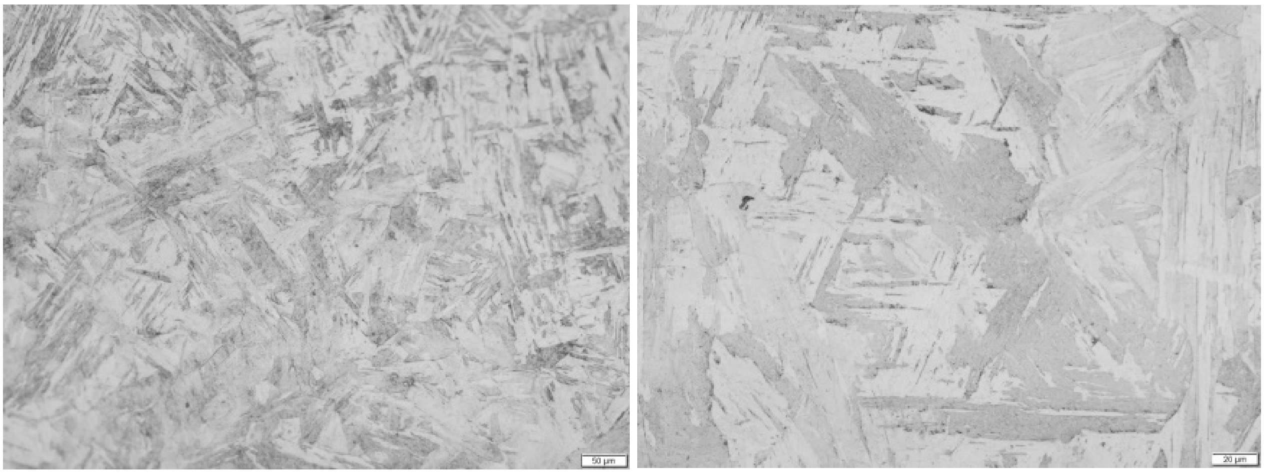

a b

Fig. 5.4 Optical microscopy images for sample 2 results after casting 200x (a) 500x (b); Marble attack reagent

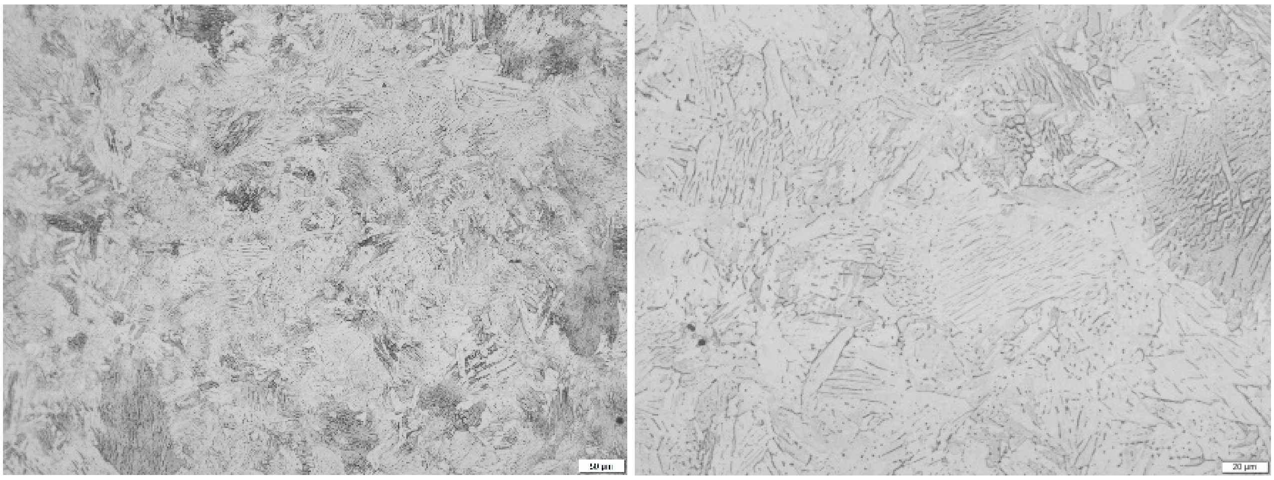

a b

Fig. 5.5 Optical microscopy images for sample 3 results after casting 200x (a) 500x (b); Marble attack reagent

In all samples, optic microscopy images at small magnification powers (200x) reveal major structures with a needle-like distribution of martensite. Middle magnification powers (500x) allow for a division of structures. In the case of samples 1 and 2 along with martensite specific structures, bright, insular, well-defined regions corresponding to the ferrite appear, confirming the ferito-martensitic structure of these steels and established their positioning of their chemical composition in the Schaeffler structural diagram. There is a slight increased proportion of ferrite in sample 2 due to the additional quantity of Mo, element α-gen, contained in this steel.

Sample 3, along with martensite formations, shows a luminous background attributed to austenite. In this case the austenitic-martensitic structure determined by the compositional position in the Schaeffler diagram is confirmed.

Regarding the specific martensite morphology, in all cases, a coarse structure, typical for the casted structures, with average lengths of martensite needles of 100 ÷ 150 µm for samples 1 and 2 and slightly less than 80 ÷ 90 µm for sample 3 It is worth mentioning Ni influence, finishing the granulation, which is specifically found in the analyzed case.

A detail to be mentioned relates to the provision of martensite needles, which form rather regions with parallel distribution and not needle orientations two by two at sharp angles. It is recognized in this morphology the "lath martensite", which in fact specifies little carbon martensite, in the case of the three studied steels.

5.3.2. Structural investigations of samples obtained after calving

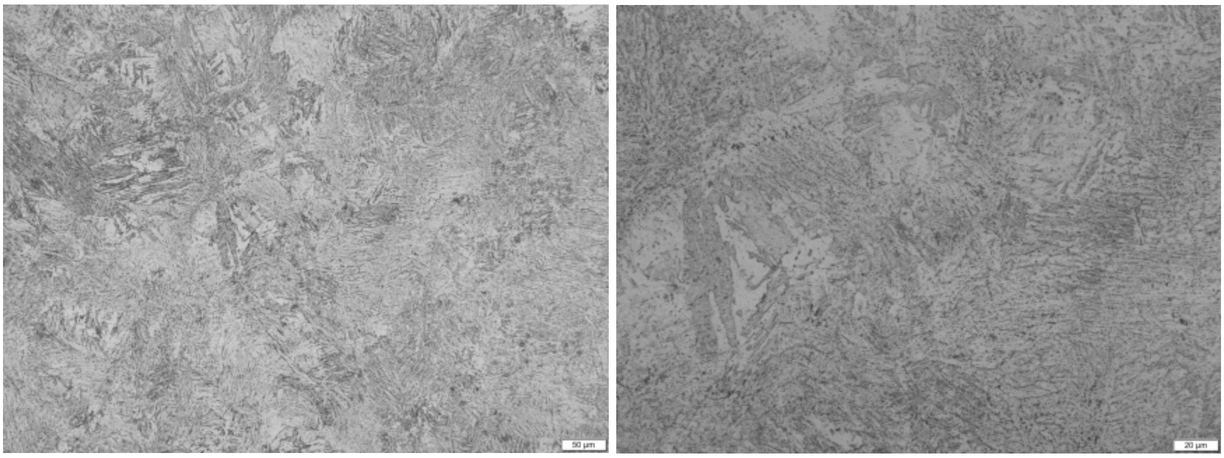

a b

Fig. 5.6 Optical microscopy images for sample 3 results after quenching (T = 1000˚C)
Magnification 200x (a) 500x (b); Marble attack reagent

Images of small scale powers (200x) of the quenched samples illustrate in all cases structures that do not differ to much from the casting structure. In both cases the structures are martensitic, which demonstrates the auto quenching character attributed to the steels.

A higher magnification power (500x) brings better structural characteristics. There is an important tendency to finishing granulation after hardening. Thus, for samples 1 and 2 the lengths of martensite needles are adjusted by reaching average dimensions of 80 ÷ 90 μm, as for sample 3, where the average length of the needles is in the range 70 ÷ 80 μm.

Hardening also has an effect on the phases accompanying martensite, in case of samples 1 and 2 the ferrite islands are reduced, and in case of sample 3 the austenitic light background becomes thinner.

All observations suggest higher mechanical properties, reinforcing the option to apply martensitic hardening after casting, even if steel is self-hardening.

5.3.3. Structural investigations of samples obtained after recovery

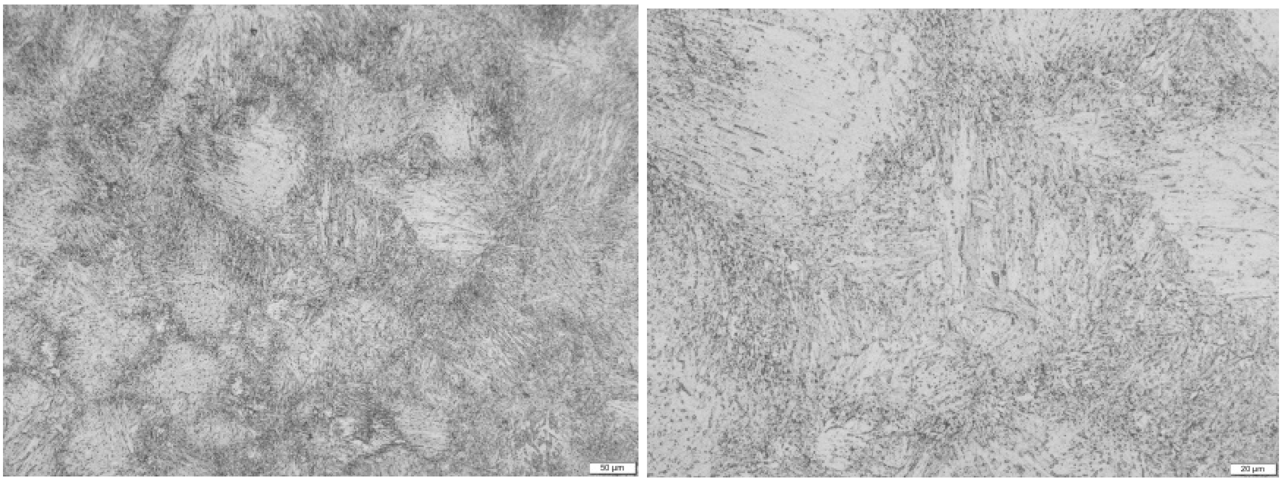

a b

Fig. 5.7 Optical microscopy images for sample 3 results after recovery (Aging T = 480˚C) Increase 200x (a) 500x (b); Marble attack reagent

Figure 5.7, corresponding to sample 3, is more special. The precipitation tendency is much more intense, highlighting the point particles that follow straight paths. A more intense precipitation predisposition can be determined by following the darker circular contours noted in both the 200x micrograph and the 500x micrograph. The stronger precipitation action in the mentioned area suggests the existence of a phasic heterogeneous micro-region, in fact an old austenitic grain boundary, in interference with martensitic formations. As is known, grain boundaries are preferential areas where diffusion takes place more intensely, facilitating the formation of new phases by precipitation in the case studied. The nature of the grain boundary or the nature of precipitations will be determined by the electron microscopy studies to follow.

5.4 Structural and compositional investigations by Scanning Electron Microscopy (SEM) associated with Energy Dispersion Spectroscopy (EDS)

Optical microscopy studies have provided a succession of data attesting the influence of the chemical composition of steels on the structure and the changes generated by heat treatments. To complete the database, more rigorous information can be provided by scanning electron microscopy studies associated with analytical electron microscopy.

5.4.1. SEM and EDS investigations on sample 3

Next, the image of secondary electrons for sample 3, the one having a special chemical composition chosen, will be presented.

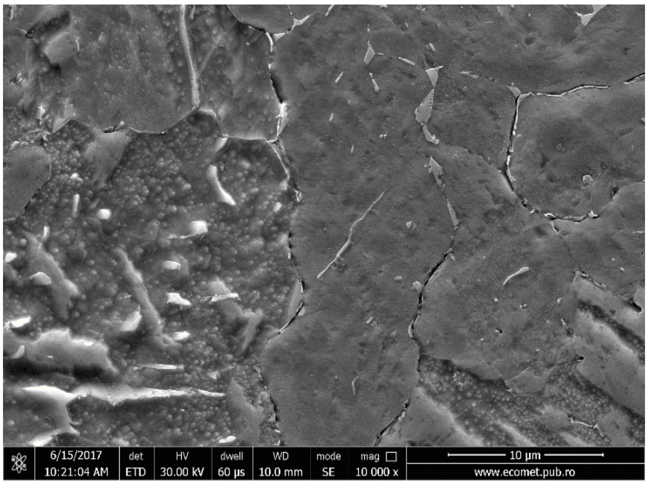

Fig. 5.8 Scanning electron microscopy (image of secondary electrons) for cast 3 sample

The detail of the predominant structure is an alternation of regions with shale, acicular distribution, with grouped punctiform points in relief. In these details, and in samples 1 and 2, the predominant martensitic structure of steel is recognized. As a comparison with the other analyzed samples, the martensite in this image is finer, more uniform, the direct consequence of the Ni presence in the chemical composition, an element known by its granulation finishing capacity.

A significant detail in the structure is the brighter islands surrounding the martensite formations. From the phase point of view, it is identified with austenite, demonstrating the biphasic (martensito-austenitic) structure resulting from the Schaeffler structural diagram. The image of secondary electrons with selected areas where the chemical composition was analyzed locally can be seen in Figure 5.9

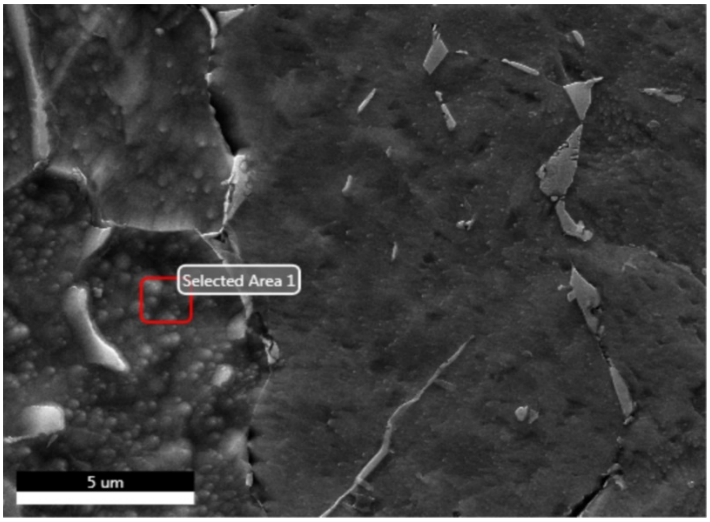

Fig. 5.9 Retrodiflowed electron image (10000x magnification) for sample 3 cast with chemical composition analysis in the selected area (1)

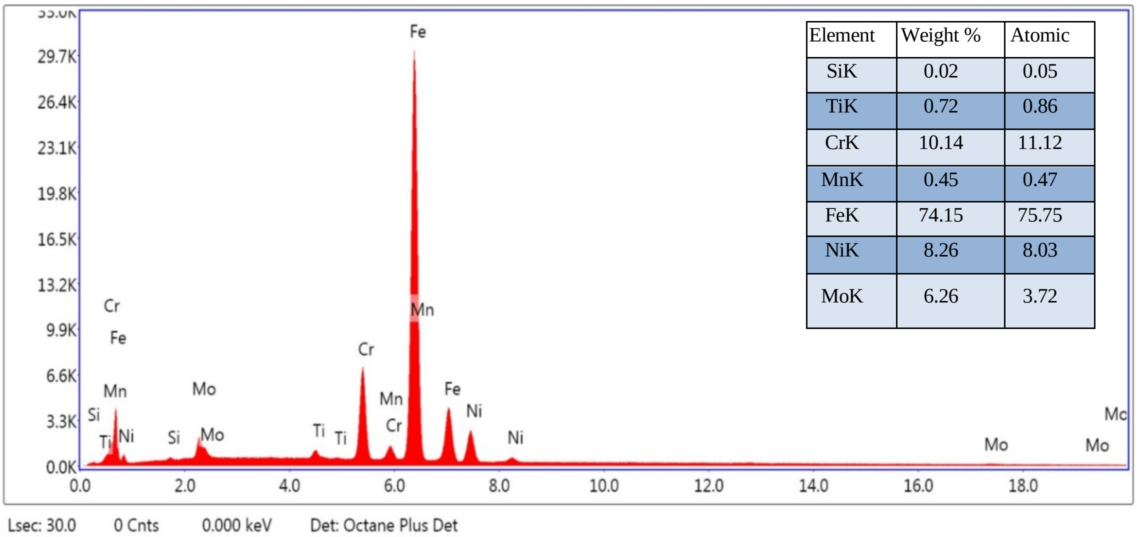

Element	Weight %	Atomic
SiK	0.02	0.05
TiK	0.72	0.86
CrK	10.14	11.12
MnK	0.45	0.47
FeK	74.15	75.75
NiK	8.26	8.03
MoK	6.26	3.72

Fig. 5.10 Spectrum EDS and chemical analysis in the selected area (1)

5.4.2. SEM investigations on quenched samples

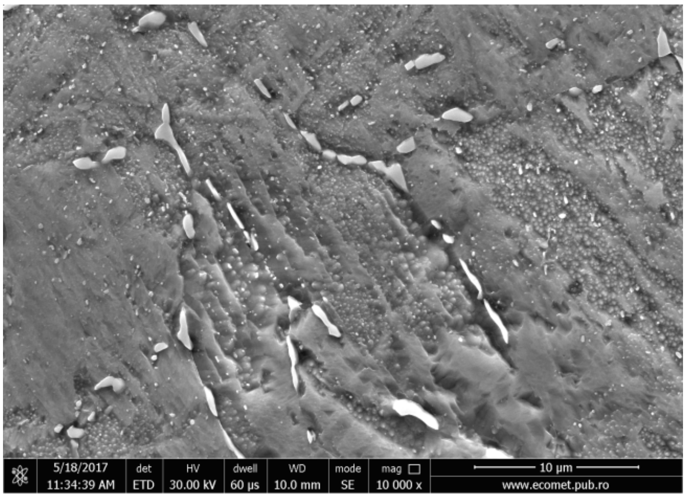

Fig. 5.11 Scanning electron microscopy (image of secondary electrons) of sample 3 (10000x magnification)

As a general observation SEM images of the qualitative samples do not differ significantly from the cast samples. Analyzed more carefully, there is a general tendency for finishing the granulation after the quenching, also visible through optical microscopy. The choice of a heating temperature for quenching according to the data in the literature for martensitic steel makes the granulation to be finished from the beginning. Further, the cooling medium, although for this category of self-hardening steels is recommended only for massive parts, proves to be favorable because the ferrite areas (sample 1 and 2) and the austenitic (sample 3) significantly decrease. The result is indeed advantageous if it is considered that tempering only the martensite through its specific transformations contributes to providing favorable mechanical resistance characteristics.

5.4.3 SEM and EDAX investigations on hardened and tempered samples

Significant changes in mechanical properties were reported after recovery. If the hardness dropped (sample 1 from 349 HV to 280 HV, sample 2 from 343 HV to 318 HV) for sample 3, the hardness increased (from 315 HV to 486 HV) for sample 3.

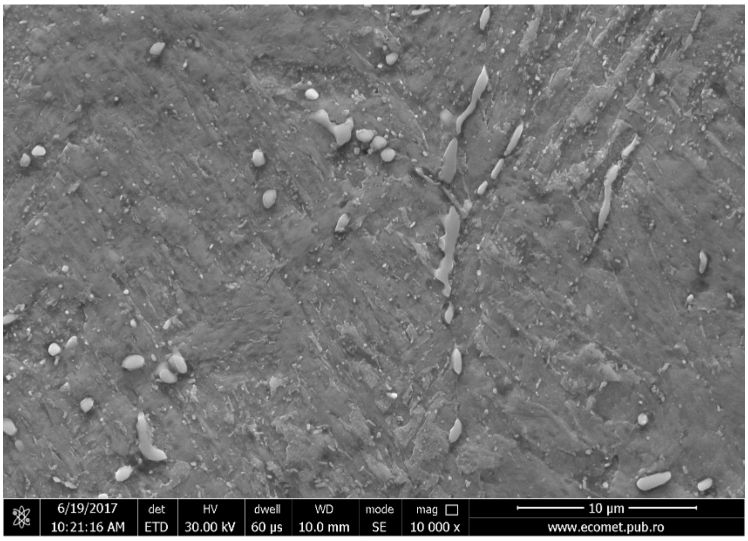

Fig. 5.12 Scanning electron microscopy (secondary electrons) for sample 3 - hardened and tempered (Magnification 10000x)

The SEM image captures a major area (fund) with acicular distribution (martensitic) with elongated (gray) areas arranged in austenite network, but also a distribution of bright globular particles with a denser distribution around martensite needles. These particles can be attributed to the specific precipitates that occur upon return. However, associating the structural results with those resulting from the hardness tests (315 HV after hardening or 486 after tempering), it can be said that the present phenomena are more specific to aging than to tempering. In fact, the chemical composition of this steel was inspired from maraging steels.

Next, the results of EDS spectroscopy and chemical analysis performed in two representative regions: in a higher homogeneity zone (zone 1), but also in an area with a density of precipitated globular particles (zone 2)

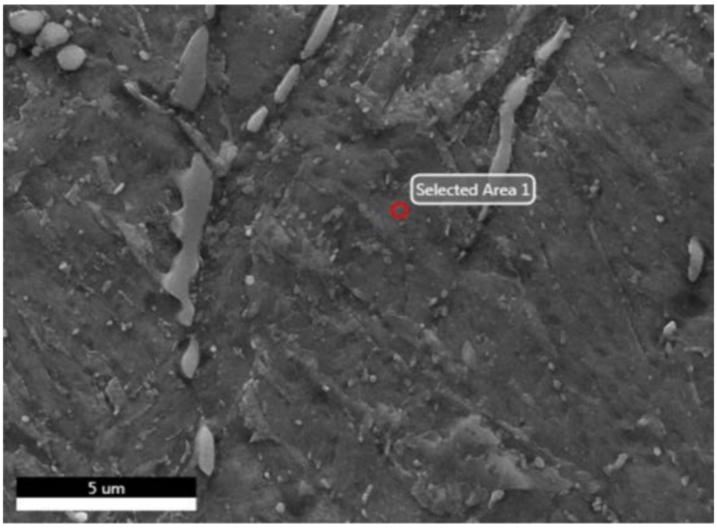

Fig. 5.13 Backscattered electrons image showing area 1 of analysis

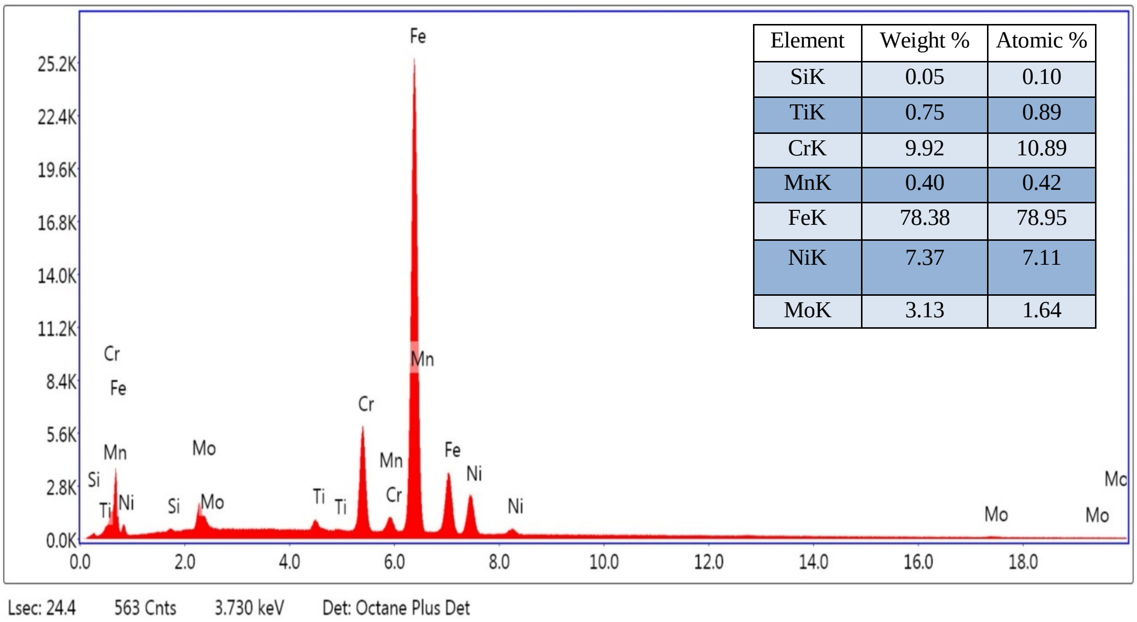

Element	Weight %	Atomic %
SiK	0.05	0.10
TiK	0.75	0.89
CrK	9.92	10.89
MnK	0.40	0.42
FeK	78.38	78.95
NiK	7.37	7.11
MoK	3.13	1.64

Fig. 5.14 EDS spectra and chemical analysis in the selected area 1

Local compositional analysis brings near-close values compared to chemical analysis through optical emission. However, Ni values may be below the mean value (7.37% vs. 10%) and Mo (3.13% vs. about 5%). Chromium remains with a close composition (9.92 vs. 10%) and Ti shows a slightly lower value (0.75% vs. 0.9%).

Chapter 6 Experimental research on cavitation and corrosion resistance of steels developed

Resistance to cavitational erosion of materials can be determined under laboratory conditions on the following types of equipment: rotary disk drip installations immersed in liquid; hydrodynamic tunnels with strangled work chamber; vibratory installations and cavitation jet installations.
The vibratory method has as main advantages the short test time and the easy possibilities of comparing the results.
The experiments performed within the ECOMET Center at the Polytechnic University of Bucharest were made using a modified version of the standardized ASTM G32 method on a piezoelectric crystal system. The change consists in positioning the specimen at a distance of 0.5 - 07 mm from the end of the sonotrode, the specimen being attached to it. The method is referred to in the literature as indirect vibration method or stationary sample vibration method. The fastening of the specimen is made by a gripping device adapted to its shape and dimensions

6.1 Apparatus used

For the experimental determinations the sonotrode from the Center for Research and Ecometallurgical Expertise - ECOMET from the University POLITEHNICA from Bucharest.
The cavitation erosion test stand within ECOMET consists of the following systems (Figure 6.1):
• Hielscher UP200St electronic ultrasonic generator;
• the oscillation system;

• Cavitant tank with cooling system (spiral of copper supplied to the public water supply system);

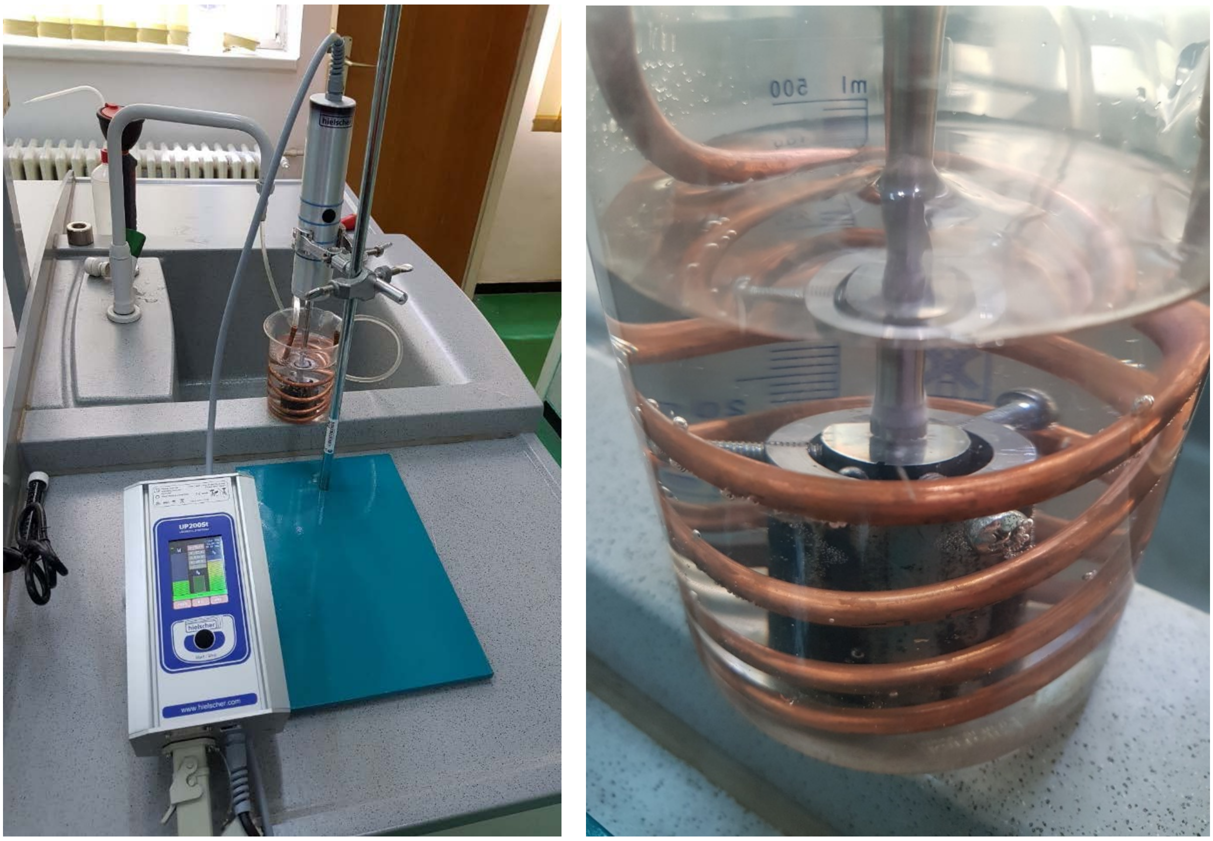

Fig. 6.1. Cavitation erosion test stand, within ECOMET

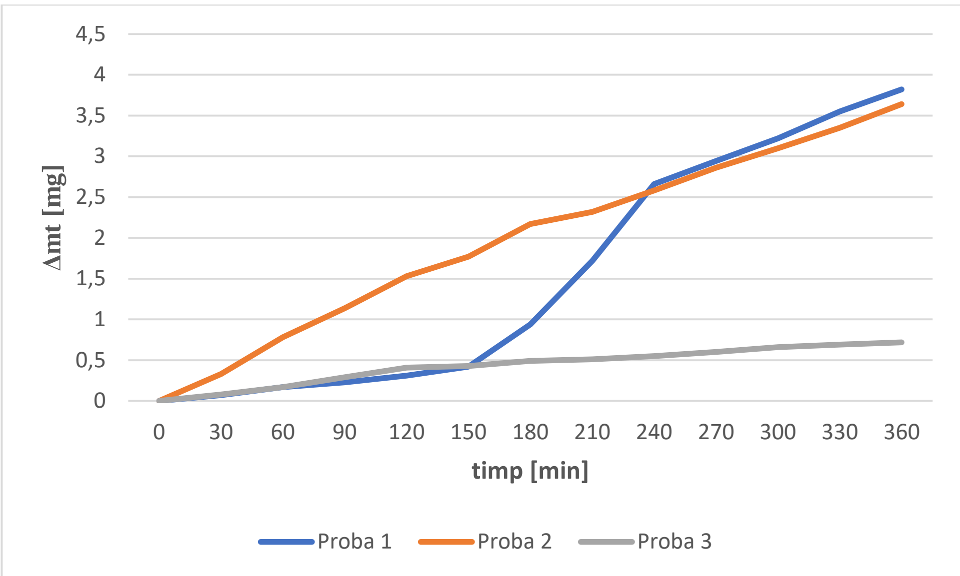

Fig. 6.2 Variation of total eroded mass at samples 1, 2 and 3

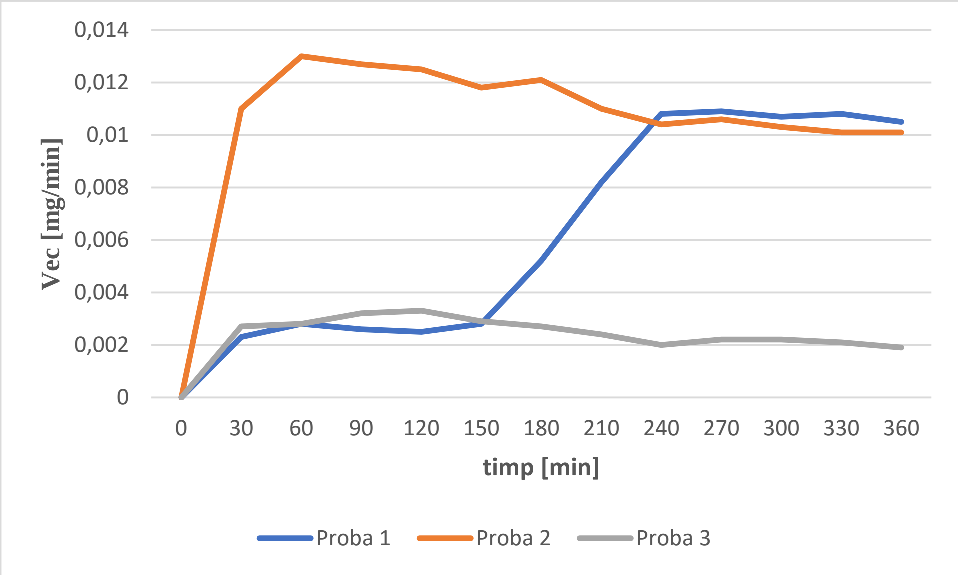

Fig. 6.3 Variation of cavitation erosion rate at samples 1, 2 and 3

Putting along the same graphs the variations in the total eroded mass we can see that the sample 2 has the highest values and shows a constant evolution, then the sample 1 has a relatively good evolution in the first half of the test after which it yields and reaches the same values with the sample 2. Unlike the first two samples, sample 3 shows a constant evolution of the eroded mass from the beginning of the test to the final, but with values much lower than the other samples, the characteristic that places it in front of them in terms of resistance to cavitational erosion.

By analyzing the curves of the cavitation erosion rate on the same graph, we can easily see that sample 2 has the highest values, then it is followed by sample 1 which has a very good resistance in the first half of the test, after which it yields and reaches the same values with sample 2. Unlike the first two samples, sample 3 shows a very low value of the cavitation corrosion rate at the beginning of the test, and tends to show decreasing values, a feature that demonstrates superiority in resistance to cavitational erosion compared to other samples.

6.2 Corrosion behavior of steels experimented in aqueous media

6.2.1 Description of the electrochemical corrosion process in aqueous media

The equipment used to analyze the corrosion behavior of steels was the Gamry Reference 600 potentiostat / galvanostat with specialized software for analyzing the data acquired by Echem Analisys as mentioned in Chapter 3. Experiments were carried out under normal ambient air conditions (22 degrees C) in freshly prepared solutions of 1N potassium sulphate and 3% NaCl. Calculation of corrosion rates was performed using the Tafel slope method.

6.2.2 Experimental results

The polarization curves for the chlorine-free aqueous medium (which is the working environment of the hydro turbines) are shown in Figure 6.4 and the polarization curves for the aqueous medium with chlorine are shown in Figure 6.5

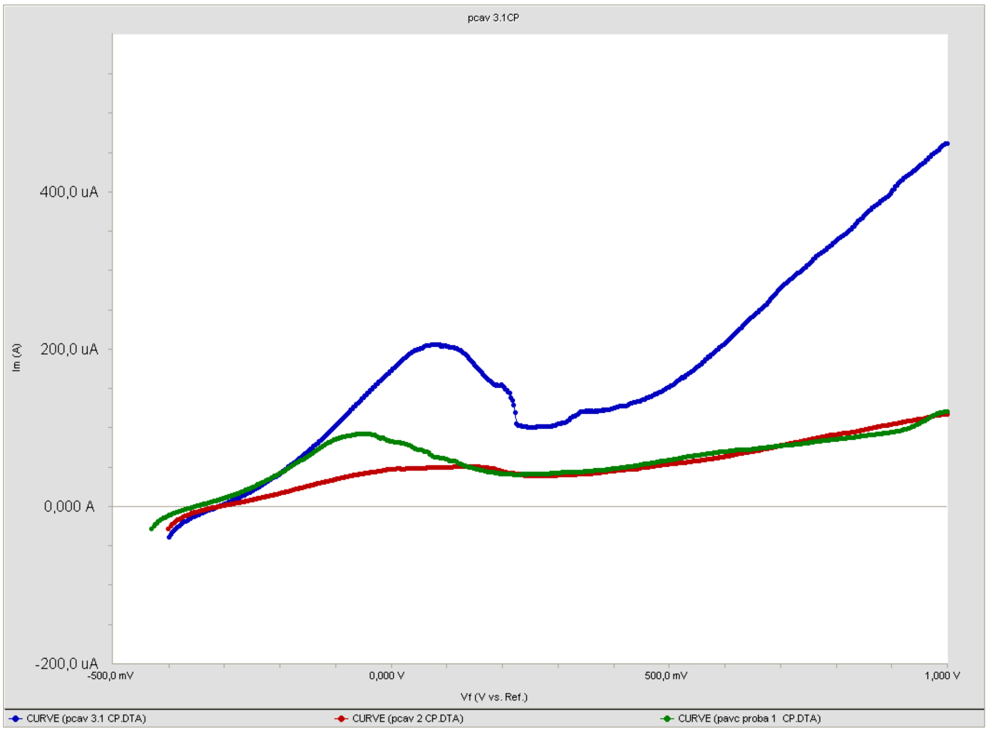

Fig. 6.4 Anodic polarization curves of the three samples traced in 1N Na2SO4 solution at ambient temperature with a polarization rate of 1mV / s

From the analysis of the anodic polarization curves shown in figure 6.4, the following aspects arise: all steels exhibit the tendency of passivation in the chlorine-free aqueous medium with the specification that the steel 3 presents an anodic field more pronounced considering the chromium content below 12% the theoretical limit for a stainless steel. The general corrosion behavior of this material is compensated by the content of about 10% Ni which leads to the martensitic major structure. Although we can not talk about proper passivation of the surface, it should be noted that the current density values are uA / cm2 for all materials including active dissolution. (maximum peak curve)

Figure 6.4 and Table 6.5 shows the results of the Tafel analysis.

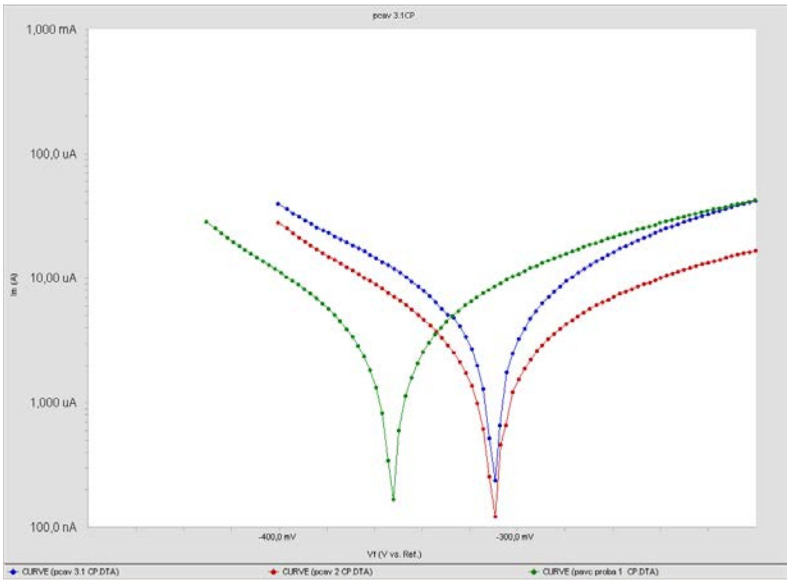

Fig. 6.5 Tafel curves plotted on the 3 samples in 1N sodium sulphate

Considering that there are no significant differences between the three materials in terms of their corrosion behavior, they were subjected to more severe conditions, namely 3% sodium chloride solution (in a first approximation it would simulate water sea).
Analysis of the material behavior in NaCl3% solution is presented in Figures 6.6 - 6.7.

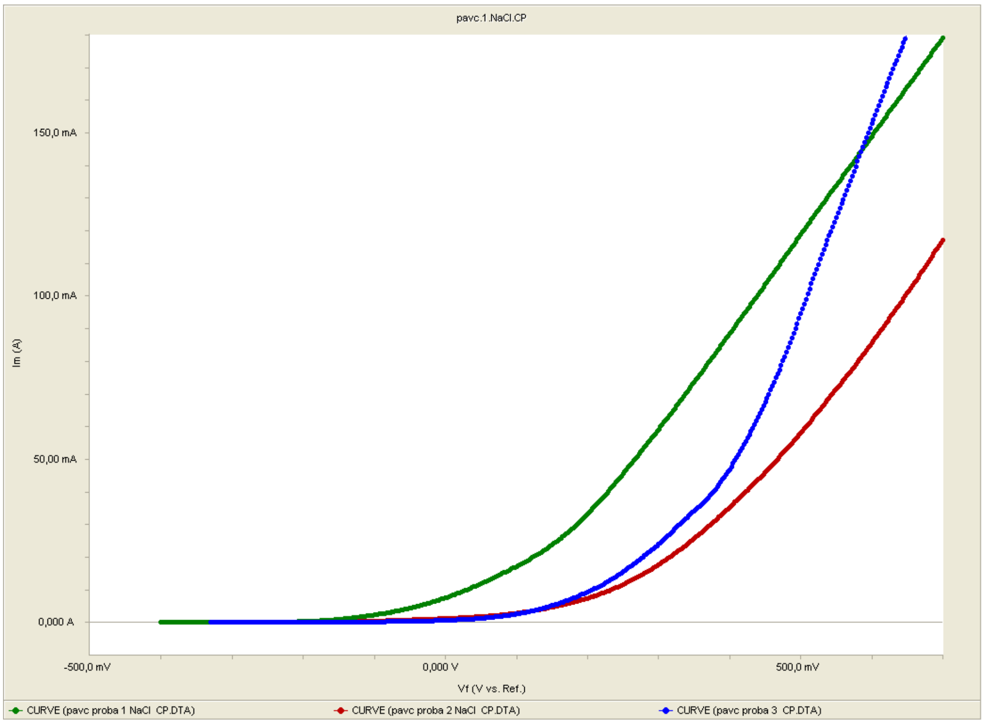

Fig. 6.6 Anodic polarization curves of the three samples traced in 1N NaCl solution at ambient temperature with a polarization rate of 1mV / s

The increased aggressiveness of the test medium and the high amount of chlorine ions prevents passivation of the surfaces, basically the corrosion current increases continuously reaching relatively high values of the mA / cm2 order and the polarization curves suddenly change the Di / Du slope to more comparative potential electronegative values with the previous medium (sulfate), and the current densities are in the order of mA / cm2. Between the steels 2 and 3 the differences are insignificant. The polarization curves overlap in a relatively broad range of potential.

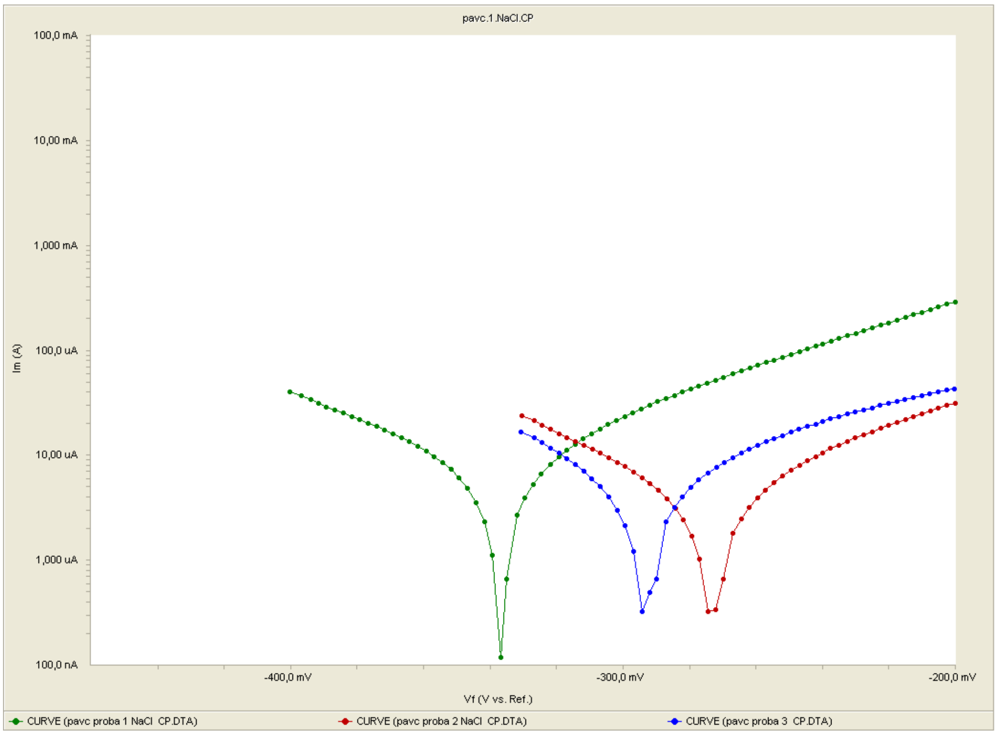

Fig. 6.7 Tafel curves plotted on the 3 samples in 3% NaCl solution

Chapter 7 Final Conclusions and Original Contributions. New research directions

7.1 Conclusions regarding the structure of the turbine blades at Izbiceni Hydro Power Plant (T8NCuMC130 CS L03.009.0 CCSIT Resita) and from Frunzaru (G-X4CrNi13-4)

7.1.1 Rotor Pallet - Izbiceni

• The chemical composition of the sample from the Izbiceni Hydro Rotor Palette corresponds to the steel mark T8NCuMC130 CS L03.009.0 CCSIT Resita, martensitic stainless steel, indicated by the literature for the execution of hydraulic turbine rotors; the presence of copper in the steel composition (Cu = 1,295) improves corrosion resistance;

• Optical microscopy examination of samples, unattacked with metallographic reagents, indicates the presence of micrometric discontinuities in the mass of the material having a circular and / or elliptical shape of variable size, randomly distributed; density of inclusions and their size is normal for the type of steel under consideration;

• Micropores were not found in the structure of the analyzed material. This indicates a superior quality of steel production and casting and has a positive influence on corrosion resistance;

7.1.2 Rotor Pallet - Frunzaru

• The chemical composition of the steel used to cast the turbine blades at Frunzaru Hydro Power Plant corresponds to a GX4CrNi13-4 EN 10283 steel grade or ASTM A743 / A743M (2003) CA6NM, martensitic stainless steel, indicated by the literature for the execution of hydraulic turbine rotors ;

• Examination by optical microscopy of the samples, unattacked with metallographic reagents, indicates the generalized presence of micrometric discontinuities in the mass of the material having a circular and / or elliptical shape of variable size, randomly distributed;

• The source of the corrosion phenomenon on the active surface of the blades is the quality of the material, respectively the existing discontinuities in its mass (inclusions, micro holes / micropores) resulting from the steel forming and casting process.

7.2 Conclusions on the determination of the chemical composition and the elaboration technique for the experimental steels

• Taking into account the causes that led to the advanced degradation due to complex cavitation and corrosion erosion of turbine blades, the principle of using competitive steels has made it essential to choose very strict conditions of elaboration, the induction furnace in the atmosphere controlled being considered the optimal method of obtaining.

• The second important step was to establish the chemical composition for the steels that were the basis of research in this study. Thus, three batches were developed, each with its specific steel:

• Sample 1 - the chemical composition of the Frunzaru palette was reconsidered, the steel finally having a martensito-ferritic structure according to the Schaeffler diagram.

• Sample 2 - A composition similar to Sample 1 but to which 1% Mo was added to increase corrosion resistance by pitting, according to the Schaeffler diagram, a martensite-ferritic structure.

• Sample 3 - An innovative composition was created. The chemical composition of sample 3 was chosen so that the interaction between the main alloying elements (Cr, Ni, Mo, Ti) leads, on the one hand, to a structural equilibrium of the two phases (ferrite, F and austenite, A) and, on the other hand, to avoid the formation of hard and fragile intermetallic compounds (Sigma σ, Chi χ, carbides, M23C6, etc.) that affect toughness and corrosion resistance. Taking into account the high mechanical stresses induced by the cavitation erosion phenomena, as well as the corrosion resistance requirements, the chemical composition was designed having the starting point of the composition of a maraging steel alloyed mainly with Ni, but without neglecting the content of Cr, responsible for increasing corrosion resistance. Titanium was another alloying element of interest known as the initiating factor in the precipitation of Ni3Me-type curative compounds. However, the titanium content has been restricted to a minimum as the formation of the Ni3Ti compound generating the highest level of hardening induces locally important internal stresses that can negatively influence corrosion resistance. The presence of titanium is beneficial to the formation of Ni3Me compound, another intermetallic phase of the same family with a durifying but slightly diminished effect that affects less corrosion resistance. According to the Schaeffler diagram, the structure is martensito-austenitic.

7.3 Conclusions on the results of investigations by optical microscopy and electron microscopy

• Optical and electronic microscopy studies on molded samples revealed similar structures within the three experienced steels. The joint structural detail is the martensitic acicular structure with typical morphology typical of all low carbon martensite. Along with martensitic distributions, luminous island islands could also be located for samples 1 and 2 or a luminous austenitic background for sample 3. These structural details confirmed the structural class identified in the Schaeffler diagram;

• The images of the qualitative evidence firstly reveal a finishing effect of the structure, the martensite assemblies become more fine. At the same time, the proportion of phases that accompany martensite (ferrite, for samples 1 and 2) and austenitic (sample 3) are reduced. All observations suggest higher mechanical properties, reinforcing the option to apply martensitic hardening after casting even if steel is self-lubricating.

• Sample 3 brings more structural aspects, demonstrating its more specific character. In micrographs (optical or electronic), there is a more intense precipitation tendency. Point chemical analysis allowed the identification of these precipitates in the form of complex intermetallic compounds whose chemical formula can be written as Ni3 (Ti, Mo). The increase in hardness after recovery from 315 HV to nearly 486 HV confirms the hardening effect of the compounds identified by hardening mechanisms by precipitation, a particular mechanism of dispersing hardening.

7.4 Conclusions on the results obtained in the cavitation erosion test

• Testing of the surfaces of the three steel samples at cavitation erosion was performed using a modified version of the standardized ASTM G32 method on a piezoelectric crystal plant. The change consists in positioning the specimen at a distance of 0.5 - 07 mm from the end of the sonotrode, the specimen being attached to it. The fastening of the specimen was made by a gripping device adapted to its shape and dimensions

• Sample 3 shows the tendency to stabilize the surface that gives the cavitational corrosion resistance as well as a lower roughness than in the case of sample 1. It can be seen that the maximum height at which the surface roughness of sample 3 comes after 6 hours of corrosion is about 800 nm, and for sample 1 under the same corrosion conditions it is 900 nm.

• Following surface and rugged AFM analysis, we can see that sample 3 shows a high resistance to cavitation corrosion and a high tendency to form a smooth and stable surface during the cavitation attack.

7.5 Conclusions on the results obtained in the electrochemical corrosion test

• Following electrochemical corrosion testing, it was found that samples 1 and 2 showed large scale attacks in the order of millimeters that seem to follow a preferential direction on the surface.

• The analysis of the anodic polarization curves reveals the following aspects: All steels exhibit the tendency of passivation in chlorine-free aqueous medium, with the specification that steel 3 presents an anodic field more pronounced considering the chromium content below 12% the theoretical limit for a stainless steel. The general corrosion behavior of this material is compensated by the content of about 10% Ni which leads to the martensitic major structure. Although we can not talk about proper passivation of the surface, it should be noted that the current density values are μA / cm2 for all materials including active dissolution. (maximum peak curve)

7.6 New research directions

Based on the results obtained in the PhD thesis, the following directions for future research can be formulated:

- Elaboration and characterization of new steels for hydroelectric turbines production;
- Development of new technologies for redevelopment of affected areas of hydroelectric turbine blades.

References

[1] Junaid, H. Masoodi, G. A. Harmain, A methodology for assessment of erosive wear on a Francis turbine runner, Energy 118 (2017) 644-657;

[5] Anant Kr. RAI, Arun KUMAR, Analyzing hydro abrasive erosion in Kaplan turbine. A case study from India, Journal of Hydrodynamics, 2016,28(5):863-872;

[9] P. Niederhofer, S.Huth, Cavitation erosion resistance of high interstitial CrMnCN austenitic stainless steels, Wear 301 (2013) 457–466;

[10] G. Bregliozzi, A. Di Schino, S.I. Ahmed, J.M. Kenny, H. Haefke, Cavitation wear behaviour of austenitic stainless steels, Wear 258 (2005) 503–510;

[14] Myung Chul Park, Gyeong Su Shin, Jae Yong Yun, Ji Haeng Heo, Dae Il Kim, Seon Jin Kim, Damage mechanism of cavitation erosion in austenite→martensite phase transformable Fe–Cr–C–Mn-Ni alloys; Wear310(2014)27–32;

[16] M. K. Padhy, R. P. Saini, Effect of size and concentration of silt particles on erosion of Pelton turbine buckets; Energy 34 (2009) 1477–1483;

[23] D. H. Mesa, C. E. Pinedo, A.P. Tschiptschin, Improvement of the cavitation erosion resistance of UNS S31803 stainless steel by duplex treatment, Surface & Coatings Technology 205 (2010) 1552–1556;

[27] Matevz Dular, Olivier Coutier Delgosha, Martin Petkovšek, Observations of cavitation erosion pit formation, Ultrasonics Sonochemistry 20 (2013) 1113–1120;

[28] B.G. Gireń, J.Frączak, Phenomenologocal prediction tool for cavitation erosion fed with the International Cavitation Erosion Test results, Wear364-365(2016)1–9;

[33] Zhen Li, JieshengHan, JinjunLu, JiansongZhou, JianminChen, Vibratory cavitation erosion behavior of AISI 304 stainless steel in water at elevated temperatures, Wear 321(2014), 33–37;

[44] N. L. Hancox and J. Brunton, The erosion of solids by the repeated impact of liquid drops, Philos. Trans. R. Sot. London, Ser. A, 260 (1966) 121-139.

[52] Takgi T, Okamura T, Sato J. Hydraulic performance of Francis turbine for sediment-laden flow, Hitachi review No-2, 1988;

[53] Krause M, Grein H. Abrasion research and prevention. Hydropower Dams 1996, 4, 17–20;

[58] Naidu BSK. Developing silt consciousness in the minds of hydropower engineers, Proc. 1st International conference on silting problems in hydropower plants, India, 1999. p. 1-36;

[59] Roman JM, Xin LY, Hui WM, Reginensi JP. Dealing with abrasive erosion in hydro turbine. Hydropower, Dams 1997,3, 67–71;

[102] Kwok, C.T., Cheng, F.T., Man, H.C., Synergistic Effect of Cavitation Erosion and Corrosion of Various Engineering Alloys in 3.5% NaCl Solution, Materials Science and Engineering, A290 © 2000.

[105] Turbine Repair, http://www.usbr.gov/power/data/fist/fist2~5/2~5_4.htm.

[106] Abood, T.H., 2008. The influence of various parameters on pitting corrosion of 316L and 202 stainless steel. In: Department of Chemical Engineering of the University of Technology. University of Technology.

[121] Melchers, R.E., 1999. Corrosion uncertainty modelling for steel structures. J. Constr. Steel Res. 52, 3-19.

[122] Schiroky, G., Dam, A., Okeremi, A., Speed, C., 2009. Pitting and Crevice Corrosion of Offshore Stainless Steel Tubing. Oil on line.
[123] Melchers, R., Ahammed, M., 1994. Nonlinear Modelling of Corrosion of Steel in Marine Environments. Department of Civil Engineering and Surveying, University of Newcastle.
[131] Nunez, M., 2007. Prevention of Metal Corrosion: New Research. Nova Publishers.
[132] Ryan, Mary P., Williams, D.E., Chater, R.J., Hutton, B.M., McPhail, D.S., 2002. Why stainless steel corrodes. Nature 415 (6873), 770-774.
[144] Friend, J.N., 1940. Deterioration of Structures of Timber, Metal, and Concrete Exposed to the Action of Sea-water.
[147] Zatkalíkov V., Bukovina, M., Skorík, V., Petrekov L., 2010. Pitting corrosion of AISI 316Ti stainless steel with polished surface. Mater. Eng. 17, 15.
[148] Thomas, C., Edyvean, R., Brook, R., 1988. Biologically enhanced corrosion fatigue. Biofouling 1, 65-77.
[154] Manning, P., Duquette, D., Savage, W., 1980. Technical Note: the effect of retained ferrite on localized corrosion in duplex 304L stainless steel. Weld. J. 59, 260-262.
[162] Sohaciu, M., Ciucă, S., Savastru D., Coman, G., Predescu A., Berbecaru, A., Cotruț, C., Matei, E., Gherghescu, I. A., Predescu, C., Influence of turbine blades fabrication conditions on their lifetime, Optoelectronics and Advanced Materials, Rapid Communications, Vol. 10, Issues 3-4, P. 257-261, 2016, Document Type: Article, WOS:000376707900027, ISSN: 1842-6573;
[171] Predescu, C., Pantilimon, C., Sohaciu, M., Matei, E., Savastru, D., Berbecaru, A ., Predescu A., Anton, MG., Coman, G., Investigation of the corrosion cracks in a C4 heavy transport pipeline by microscopy, fluorescence and diffraction techniques, Journal of Optoelectronics and Advanced Materials, vol. 18, issue 9-10, p. 873-877, 2016;
[172] G. Coman, S. Ciucă, A. C. Berbecaru, M. C. Pantilimon, M. G. Sohaciu, C. Grădinaru, C. Predescu, 2017, New Martensitic Stainless Steel Hardenable by Precipitation for Hydropower Turbines, U.P.B. Sci. Bull., Series B, Vol. 79, Iss. 4, ISSN 1454-2331;